[redacted]

NACA RM L52D22

NACA

RESEARCH MEMORANDUM

A METHOD FOR ESTIMATING THE COMPONENTS OF LIFT OF WING-BODY COMBINATIONS AT SUPERSONIC SPEEDS

By Warren A. Tucker

Langley Aeronautical Laboratory
Langley Field, Va.

[redacted]

NATIONAL ADVISORY COMMITTEE
FOR AERONAUTICS

WASHINGTON

September 16, 1952

[redacted]

NATIONAL ADVISORY COMMITTEE FOR AERONAUTICS

RESEARCH MEMORANDUM

A METHOD FOR ESTIMATING THE COMPONENTS OF LIFT OF WING-BODY COMBINATIONS AT SUPERSONIC SPEEDS

By Warren A. Tucker

SUMMARY

The lift of wing-body combinations at supersonic speeds is obtained by means of an approximate linearized-theory analysis which involves an assumption concerning the geometry of the body. Rectangular and triangular wing plan forms are treated; the wing and body may be at different angles of attack. Also, the body may end at the wing trailing edge or may extend farther back. The results are given in the form of simple generalized curves from which the lift of any specific configuration is readily obtained.

A comparison with several groups of experimental data is presented to show that the method predicts, with acceptable accuracy, the lift on the wing and on the body.

A question proposed by Ferrari concerning the optimum wing incidence for minimum total drag is investigated; it appears that, at moderate or high supersonic speeds, wing incidence is of little value in reducing the total drag.

Several charts are presented to show how the several components of the total lift are distributed.

INTRODUCTION

In the past few years, the problem of the lift of wing-body configurations flying at supersonic speeds has been considered by several authors, who have approached the problem in different ways. Spreiter (ref. 1) has given the solution for low-aspect-ratio triangular wings mounted on slender bodies which end at the trailing edge of the wing. Ferrari (refs. 2 and 3) has developed an iteration method applicable to rectangular wings mounted on bodies which may extend behind the wing trailing edge. Ferrari's work is notable for being the only one that

treats rigorously the lift on the part of the body behind the wing trailing edge (commonly called the afterbody). Although the method in principle requires iteration, apparently the first step in the calculation procedure may give an answer accurate enough for engineering use (see refs. 3 and 4). Even with this simplification, however, and in spite of the fact that some shortening of the numerical calculations is possible (ref. 5), the work involved in the first step of the iteration process is still sufficient to make Ferrari's method one which is adapted better to the intensive investigation of the details of a particular configuration than to the examination of the over-all characteristics of a wide range of configurations.

A more recent contribution has been made by Nielsen and Pitts (ref. 6). This work includes an exact solution, within the framework of the linear theory, for the pressure distribution due to unit angle of attack of the wing of a rectangular wing-body combination. The field of application of this method is similar to that of Ferrari's.

An approximate method of wider scope has been proposed by Morikawa in reference 7. By considering limiting cases, and by making assumptions concerning the pressures on the body and on the wing, Morikawa finds the integrated lift on the wing and on the body for a wide range of parameters. He presents results for wings of rectangular, delta, and clipped-delta plan forms but considers only those cases in which the body is at the same angle of attack as the wing and extends no farther back than the wing trailing edge (no afterbody). As Morikawa points out, such an analysis should have experimental verification before being too widely applied.

The present contribution is also an approximate method but is based on different assumptions from those used by Morikawa. The principal assumption is that the body can be replaced by a flat plate in the plane of the wing; the lift on the wing and on the body of the resulting planar configuration are then readily calculated by standard methods. The method is applied to configurations having wings of either rectangular or triangular plan form, which may be at a different angle of attack from the body. The effect of the afterbody is also treated in an approximate manner, so that the body may end at the trailing edge of the wing (no afterbody) or may extend farther back. A correlation is made with available experimental data in order to assess the validity of the simplifying assumptions.

While the present work was being completed, another approximate method proposed by Nielsen and Kaatari (ref. 8) became available. In that paper, the lift on the wing is estimated by a modification of slender-body theory (ref. 1). In order to estimate the lift on the body, the body is imagined to be collapsed to a flat plate, as in the present paper, but only the lift on the body due to wing angle of attack

is considered; the lift on the body due to the wing in the presence of the body upwash is neglected. The effect of an afterbody is approximated in the same general manner as in the present paper, with a slightly greater effective area being used. The method is applied to configurations having wings of rectangular, triangular, or trapezoidal plan form at the same angle of attack as the body. A comparison with a large number of experimental data is presented to show that the method predicts very closely the total lift of wing-body combinations. The method has also been used to predict the division of lift between wing and body, but the results are not yet available in published form.

SYMBOLS

a	body radius
s	wing semispan
c	wing root chord
m	slope of wing leading edge (see fig. 2)
x,y	rectangular coordinates for field points
ξ,η	rectangular coordinates for source points
S_e	exposed wing area
V	free-stream velocity
q	free-stream dynamic pressure
M	free-stream Mach number
$\beta \equiv \sqrt{M^2 - 1}$	
α_W	wing angle of attack
α_B	body angle of attack
α_u	upwash angle
i_W	wing angle of incidence, $\alpha_W - \alpha_B$
w	upwash velocity
$w_B \equiv \alpha_B V$	

φ velocity potential

C_{L_W} wing lift coefficient, $\frac{\text{Lift on wing}}{qS_e}$

C_{L_B} body lift coefficient, $\frac{\text{Lift on body}}{qS_e}$

C_D drag coefficient, $\frac{\text{Drag}}{qS_e}$

A aspect ratio of rectangular wing, $\frac{2s}{c}$

All angles are in radians, unless otherwise specified.

ASSUMPTIONS AND METHOD

At the outset, the original problem was broken down into three separate parts, as proposed in reference 9 by Lagerstrom and Van Dyke (see fig. 1). In figure 1, the lift of the complete configuration, with the wing at an angle of attack α_W and the body at an angle of attack α_B, is shown as equal to the lift of the isolated body plus the lift of the two configurations on the right-hand side of the figure. In each of these two configurations the body is at zero angle of attack and extends to infinity ahead of the wing; in the one case the wing is at an angle of attack α_W, and in the other case the angle of attack varies with the spanwise position along the wing, being equal to α_u, the upwash-angle distribution around the isolated body at angle of attack α_B. If the body is assumed to be approximately cylindrical from the trailing edge of the wing to a point far enough ahead of the wing so that the influence of the body nose can be considered negligible, then in the notation of figure 2 the upwash angle has been shown by Beskin in reference 10 to be given by the following equation:

$$\alpha_u = \frac{\alpha_B}{\left(1 + \frac{y}{a}\right)^2} \tag{1}$$

The lift of the isolated body can be assumed known (ref. 11 or 12), so that the remaining problem is to find the lift on the wing and on the body of the two configurations at the right-hand side of figure 1. It

is remarked that within the framework of the linearized theory the superposition scheme shown in figure 1 is not an approximation but is exact in the sense that the sum of the solutions to the three subproblems is the complete solution and requires no iteration. The purpose of the scheme is to simplify the total problem by means of a breakdown into several basic problems.

The remaining problem is now considered. A rigorous solution (except for Ferrari's iteration method and the work described in ref. 6) has so far not been published and when it is found it will almost certainly be of such a length that, like Ferrari's solution, it will be best adapted to detailed analysis of a particular configuration rather than to a broad examination of the field. Therefore, in order to obtain useful approximate values for the lift on the wing and on the body, two assumptions are made. The first of these assumptions is that the cylindrical body can be replaced by a flat plate in the plane of the wing (but the upwash is still taken to be that around the cylindrical body). This assumption, of course, violates physical reality because the boundary condition on the true body surface is no longer met; the success of the approximation is best judged by a later comparison with experimental results. The second assumption, which is necessary only when the body extends behind the trailing edge of the wing, is that the lift on the body is confined within the area shown in figure 3. This assumption is again only an approximation to the actual situation, as can be seen by an examination of the data of reference 13, for example.

The reason for making each of these approximations is the same; namely, to simplify the problem to the extent that useful approximate answers can be obtained without excessive calculation for fairly extensive ranges of the variables involved. In the present case, the lift on the body and on the wing was determined in the following manner. The wing-body combination was represented by a source distribution appropriate to each case (rectangular or triangular wing and wing angle of attack given by α_w or α_u), and the velocity potential in each of the several pertinent areas, taking due account of the tip effect where present, was determined by the methods of Puckett and Evvard (refs. 14 and 15). The potential in each area was then evaluated at the downstream limit of the area; this step resulted in the spanwise lift distribution, which was then integrated (in most cases numerically) over the wing and over the body to give the net lift on each component. A typical case which illustrates the procedure is described in the appendix.

PRESENTATION OF RESULTS

Calculations have been made, by the procedure described previously, of the lift on the wing and on the body for configurations having rectangular and triangular wings. The results were obtained in the form of generalized lift-curve slopes as functions of the generalized wing plan-form variable βA (for rectangular wings) or βm (for triangular wings), with the body-wing size ratio a/s as a parameter. For a particular value of a/s, the calculations were carried out only for values of βA or βm greater than a certain minimum value determined by the position of the Mach line from the leading point of the wing-body juncture relative to the body or to the wing tip (for the rectangular wing only). The limiting cases are shown in figure 4.

The results of the calculations are presented in figures 5, 6, and 7 for the rectangular-wing case and in figures 8, 9, and 10 for the triangular-wing case. The curves for the triangular-wing case have been extrapolated past the limit shown in figure 4 to $\beta m = 0$, as indicated by the dashed parts of the curves. In most cases the method of extrapolation is obvious; in the case of figures 8(a) and 9(a) the fairing was guided by reasoning concerning the qualitative manner in which the lift is divided between the wing and the body for combinations of βm and a/s outside the limit of figure 4(b). The fairing is best justified by the later comparison with experimental data, where for some points the faired parts of the curves were used. In each figure the following components are presented:

$\frac{\beta C_{L_W}}{\alpha_W}$ the lift on the wing due to wing angle of attack

$\frac{\beta C_{L_W}}{\alpha_B}$ the lift on the wing due to body upwash

$\frac{\beta C_{L_B}}{\alpha_W}$ the lift on the body due to wing angle of attack

$\frac{\beta C_{L_B}}{\alpha_B}$ the lift on the body due to the wing in the presence of the body upwash

The origin of these four components is evident from an inspection of the two configurations at the right-hand side of figure 1. The lift components are presented in this manner in order to preserve the generality of separate angles of attack for the wing and body. The

total lift for each part of the configuration is found by simply adding the components. Thus, if $C_{L_{W(B)}}$ is defined as the total lift coefficient acting on the wing in the presence of the body, then

$$C_{L_{W(B)}} = \frac{1}{\beta}\left(\alpha_W \frac{\beta C_{L_W}}{\alpha_W} + \alpha_B \frac{\beta C_{L_W}}{\alpha_B}\right) \tag{2}$$

and if $C_{L_{B_\infty(W)}}$ is defined as the total lift coefficient acting on the semi-infinitely long body in the presence of the wing, then

$$C_{L_{B_\infty(W)}} = \frac{1}{\beta}\left(\alpha_W \frac{\beta C_{L_B}}{\alpha_W} + \alpha_B \frac{\beta C_{L_B}}{\alpha_B}\right) \tag{3}$$

If the body is not semi-infinitely long, then to $C_{L_{B_\infty(W)}}$ must be added $C_{L_{B_o}}$, the lift of the isolated body. Thus, if $C_{L_{B(W)}}$ is defined as the total lift acting on the finite body in the presence of the wing, then

$$C_{L_{B(W)}} = \frac{1}{\beta}\left(\alpha_W \frac{\beta C_{L_B}}{\alpha_W} + \alpha_B \frac{\beta C_{L_B}}{\alpha_B} + \alpha_B \frac{\beta C_{L_{B_o}}}{\alpha_B}\right) \tag{4}$$

Values for $\frac{\beta C_{L_{B_o}}}{\alpha_B}$, calculated for a body lift-curve slope of 2 based on body base area (refs. 11 and 12), are given in figure 11. This figure merely changes the reference area from the body base area to the exposed wing area, the reference area for all lift coefficients presented in this paper.

COMPARISON WITH EXPERIMENTAL DATA

The experimental data available for comparison with the calculated results are by no means numerous but they are sufficient to permit some comparison. In view of the fact that the data from the various sources are not all presented in the same form and are not equally complete (in

some cases tests have been made at only one Mach number, in other cases not all the components of lift have been measured) several groups of data are discussed separately. Insofar as is feasible, each group of data is presented in its original form.

Langley 9-inch supersonic-tunnel data.- Although this series of tests has not yet been completed, some of the results have been made available to the author in unpublished form. Briefly, the investigation consists of tests at three Mach numbers of ten wings (three rectangular and seven triangular) and a single body, tested alone and in combination. In addition to measurements of total lift, the lift on the wing in the presence of the body is measured by an internal balance. For the triangular-wing case this is the only measurement that is yet available; measurements for the rectangular-wing case are complete. Each test was made at two values of Reynolds number, but the scale effect was small. The data presented herein are for the higher Reynolds number.

The experimental and estimated results for the rectangular-wing case are compared in figures 12, 13, and 14. The lift coefficients are based on total wing area and the lift-curve slopes are per degree measure. The quantities compared are identified in the (a) part of each figure. The agreement in most cases is acceptable.

The comparison for the triangular-wing case is shown in figures 15 and 16. The lift coefficients for this case are based on exposed wing area. The agreement is satisfactory.

Sparrow missile data.- These data were obtained from tests of a 13.5-percent-scale model of the Sparrow 13-D (XAAM-N-2) air-to-air missile at the Ordnance Aerophysics Laboratory at Daingerfield, Texas and have been presented in reference 16. Both the wing and the tail of the Sparrow missile are triangular but have different apex angles. The test program, which covered a range of Mach numbers from 1.5 to 2.5, included tests of the body-plus-wing and the body-plus-tail configurations and it is the data from these tests which are compared with the present estimates. Forces were measured on the body alone, on each combination (body plus wing and body plus tail), and on the wing in the presence of the body. For the body-plus-wing configuration, tests were made not only with the body at the same angle of attack as the wing but also with the body fixed at zero angle of attack while the wing angle of attack was varied.

The appropriate comparisons are made in figures 17 and 18. All coefficients are based on the exposed area of the wings and the lift-curve slopes are per degree measure. In figure 17 the lift of the isolated body has been subtracted from the measured forces where appropriate. The agreement is, in general, satisfactory; the correlation

for the body-plus-tail configuration offers some hope that the method of estimation may work for configurations with no afterbody, and the results for the forces on the wing in the presence of the body show that the method fairly estimates the division of load. In addition, the acceptable agreement for the variable- and fixed-incidence cases indicates that the effect of the body upwash on the wing and on the body is correctly estimated.

Other data.- The foregoing groups of data are the only ones available that are sufficiently complete to permit a direct comparison of estimated and measured interference effects and components of lift. There are other data, however, for the total lift of bodies and wings in combination and the lift estimated by the present method can be compared with the measured values. Such a comparison, of course, is not so valuable as the preceding ones, but it does provide a check on the usefulness of the method for estimating over-all lift. The data presented in reference 8 and references 16 to 27 have been compared with the estimated values of total lift and the results are shown in figures 19 and 20. For consistency, all lift coefficients have been based on exposed wing area and the lift-curve slopes are per degree measure. The comparison is shown both including and excluding the lift of the isolated body, since in a strict sense the estimation of this quantity is not a part of the wing-body interference problem. For most of the cases the correlation is satisfactory, although there is a tendency for the estimated values to be low, particularly for the triangular-wing configurations.

DRAG DUE TO LIFT

An interesting problem was posed by Ferrari in reference 2; namely, what value of wing incidence will produce the minimum total drag for a given lift coefficient of the wing-body system? A related question, of course, is the following: By what percentage may the drag be reduced by using the optimum value of wing incidence? Ferrari worked out the answer for a particular configuration in reference 2 but the numerical results are not applicable because of an error (later corrected in ref. 3) in one of the boundary conditions.

The following results are obtained by following an analysis similar to that given by Ferrari in reference 2. The part of the total drag which is due to lift is given by the following equation:

$$\frac{1}{\beta}\frac{\Delta C_D}{C_L^2} = a_1\alpha_B^2 + a_2\alpha_B\alpha_W + a_3\alpha_W^2 \qquad (5)$$

The optimum values of the wing and body angles of attack are given by the following equations:

$$\frac{\alpha_W}{\beta C_L} = \frac{1}{2a_4} \frac{2a_1a_5 - a_2}{a_1a_5^2 - a_2a_5 + a_3} \tag{6}$$

$$\frac{\alpha_B}{\beta C_L} = \frac{1}{a_4} - a_5 \frac{\alpha_W}{\beta C_L} \tag{7}$$

and the wing angle of incidence is by definition

$$\frac{i_W}{\beta C_L} = \frac{\alpha_W}{\beta C_L} - \frac{\alpha_B}{\beta C_L} \tag{8}$$

where

$$\left.\begin{aligned}
a_1 &= \frac{\beta C_{L_{B_o}}}{\alpha_B} + \frac{\beta C_{L_B}}{\alpha_B} \\
a_2 &= \frac{\beta C_{L_W}}{\alpha_B} + \frac{\beta C_{L_B}}{\alpha_W} \\
a_3 &= \frac{\beta C_{L_W}}{\alpha_W} \\
a_4 &= \frac{\beta C_{L_{B_o}}}{\alpha_B} + \frac{\beta C_{L_B}}{\alpha_B} + \frac{\beta C_{L_W}}{\alpha_B} \\
a_5 &= \frac{\frac{\beta C_{L_B}}{\alpha_W} + \frac{\beta C_{L_W}}{\alpha_W}}{\frac{\beta C_{L_{B_o}}}{\alpha_B} + \frac{\beta C_{L_B}}{\alpha_B} + \frac{\beta C_{L_W}}{\alpha_B}}
\end{aligned}\right\} \tag{9}$$

The preceding relations were used with the data presented in figures 6, 8, and 9 to determine the optimum angles of incidence for two series of wing-body combinations. One series had rectangular wings and the other had triangular wings; both had long afterbodies. The results are presented in figure 21. The most obvious conclusion that might be drawn is that only at low values of βA or βm (which, for a given physical configuration, correspond to low-supersonic Mach numbers) and for bodies that are large relative to the wings (high a/s values) is the optimum incidence angle positive. However, the actual values of the optimum angles are very small. For example, at a Mach number of 2.0 and a lift coefficient of 0.1, a value of $i_W/\beta C_L$ equal to 0.1 corresponds to an incidence angle of about 1°. Furthermore, calculations of the actual drag for the optimum configurations showed that the reduction in drag was never greater than 1 percent of the drag due to lift for the corresponding zero-incidence configurations. The final conclusion, therefore, is that at moderate or high values of supersonic Mach number wing incidence is of little value in reducing the total drag.

DIVISION OF LIFT

The manner in which the total lift is distributed is of prime interest in the wing-body problem. The data presented in figures 5 to 11 have been used to find the division of lift for wing-body combinations with rectangular and triangular wings at zero incidence for two values of the parameters βA and βm, respectively, and the results are shown graphically in figures 22 to 25. Certain general features are demonstrated by both the rectangular-wing and the triangular-wing configurations; namely, that relatively more of the total lift is carried by the body for the higher values of βA or βm, that the interference lift on the body is relatively less for these higher values of βA or βm, and that the interference lift on the wing is primarily a function only of the relative body size a/s.

The interference lift as a fraction of the total lift may also be examined without regard to the division between wing and body; this form of presentation is shown in figures 26 and 27. Again the rectangular-wing and triangular-wing configurations exhibit the same general characteristics: The interference effect is relatively greater for long-afterbody configurations and for low values of βA or βm, and the value of the relative body size a/s at which the interference effect is greatest is larger for low values of βA or βm.

CONCLUDING REMARKS

A simple method is described for estimating the lift at supersonic speeds of wing-body combinations having rectangular or triangular wings. The body may extend behind the wing trailing edge and the wing may be at a different angle of attack from the body.

The results obtained are compared with experimental data; good agreement is shown. The results are then used to show that, at moderate or high supersonic speeds, the use of wing incidence is of little help in reducing the total drag. The relative values of the different components of the total lift are shown in a series of figures.

Langley Aeronautical Laboratory
National Advisory Committee for Aeronautics
Langley Field, Va.

APPENDIX

LIFT ON TRIANGULAR WING DUE TO BODY UPWASH FOR $\beta m < 1$

The first step in determining the lift on a triangular wing due to body upwash is to find the velocity potential φ at any point on the wing or (flat) body surface. The methods of references 14 and 15 are used and the setup for the necessary integration is shown in figure 28.

The potential is given by the following equation:

$$-\frac{\pi\varphi}{w_B a^2} = \int_0^{\frac{m(x+\beta y)}{1+\beta m}} \frac{d\eta}{(a+\eta)^2} \int_{\frac{1-\beta m}{1+\beta m}(x+\beta y)+\beta\eta}^{x+\beta(y-\eta)} \frac{d\xi}{\sqrt{(x-\xi)^2 - \beta^2(y-\eta)^2}} \tag{A1}$$

which when integrated gives the following result:

$$-\frac{\pi\varphi}{w_B a} = \frac{\gamma}{1+\gamma} \cosh^{-1}\left|\frac{\left(\frac{x}{c} - \frac{a}{s}\gamma\right) + \left(\frac{x}{c} + \beta m \frac{a}{s}\gamma\right)}{\frac{a}{s}(1+\beta m)\gamma}\right| +$$

$$\frac{\sqrt{\frac{x}{c} - \frac{a}{s}\gamma}}{(1+\gamma)\sqrt{\left(\frac{x}{c} + \beta m \frac{a}{s}\gamma\right) + \frac{a}{s}(1+\beta m)}} \cosh^{-1}\left|\frac{2\left(\frac{x}{c} + \beta m \frac{a}{s}\gamma\right) + \frac{a}{s}(1+\beta m)}{\frac{a}{s}(1+\beta m)}\right| \tag{A2}$$

where

$$\gamma \equiv \frac{y}{a}$$

Now the spanwise lift distribution on the wing is given by the following expression:

$$\frac{\pi V}{4qw_B a^2}\frac{dL}{dy} = -\frac{\pi\varphi_{TE}}{w_B a} \equiv \Phi \tag{A3}$$

where φ_{TE} is the velocity potential evaluated at the wing trailing edge.

The total lift on one exposed wing panel is the following:

$$\frac{L}{q\alpha_B} = \frac{4a^2}{\pi}\int_0^{\frac{1-\frac{a}{s}}{a/s}} \Phi \, d\gamma \tag{A4}$$

$\left(\text{since } \frac{w_B}{V} = \alpha_B\right)$ and the lift coefficient becomes

$$\frac{C_{L_W}}{\alpha_B} = \frac{2L/q\alpha_B}{S_e} = \frac{8m}{\pi}\left(\frac{a/s}{1-\frac{a}{s}}\right)^2\int_0^{\frac{1-\frac{a}{s}}{a/s}} \Phi \, d\gamma \tag{A5}$$

or

$$\frac{\beta C_{L_W}}{\alpha_B} = \frac{8}{\pi}\beta m\left(\frac{a/s}{1-\frac{a}{s}}\right)^2\int_0^{\frac{1-\frac{a}{s}}{a/s}} \Phi \, d\gamma \tag{A6}$$

and when Φ is evaluated from equation (A2), then the final expression for the lift coefficient on the wing results:

$$\frac{\beta C_{L_W}}{\alpha_B} = \frac{8}{\pi}\beta m\left(\frac{a/s}{1-\frac{a}{s}}\right)^2 \int_0^{\frac{1-\frac{a}{s}}{a/s}} \left[\frac{\gamma}{1+\gamma}\cosh^{-1}\left|\frac{2\left(1-\frac{a}{s}\right)-\frac{a}{s}(1-\beta m)\gamma}{\frac{a}{s}(1+\beta m)\gamma}\right| + \right.$$

$$\left. \frac{\sqrt{1-\frac{a}{s}-\frac{a}{s}\gamma}}{(1+\gamma)\sqrt{1+\beta m\,\frac{a}{s}(1+\gamma)}}\cosh^{-1}\left|\frac{2-\frac{a}{s}(1-\beta m)+2\beta m\,\frac{a}{s}\gamma}{\frac{a}{s}(1+\beta m)}\right|\right] d\gamma \quad (A7)$$

This expression was evaluated numerically to give the curves shown in figure 8(b).

REFERENCES

1. Spreiter, John R.: The Aerodynamic Forces on Slender Plane- and Cruciform-Wing and Body Combinations. NACA Rep. 962, 1950.

2. Ferrari, Carlo: Interference between Wing and Body at Supersonic Speeds - Theory and Numerical Application. Jour. Aero. Sci., vol. 15, no. 6, June 1948, pp. 317-336.

3. Ferrari, Carlo: Interference between Wing and Body at Supersonic Speeds - Note on Wind-Tunnel Results and Addendum to Calculations. Jour. Aero. Sci., vol. 16, no. 9, Sept. 1949, pp. 542-546.

4. Cramer, R. H.: Interference between Wing and Body at Supersonic Speeds - Theoretical and Experimental Determination of Pressures on the Body. Jour. Aero. Sci., vol. 18, no. 9, Sept. 1951, pp. 629-632.

5. Scheuing, Richard A.: The Lift of Wing-Body Combinations Traveling at Supersonic Speeds. Rep. No. RE-25, Grumman Aircraft Eng. Corp., July 17, 1949.

6. Nielsen, Jack N., and Pitts, William C.: Wing-Body Interference at Supersonic Speeds with an Application to Combinations with Rectangular Wings. NACA TN 2677, 1952.

7. Morikawa, George: Supersonic Wing-Body Lift. Jour. Aero. Sci., vol. 18, no. 4, Apr. 1951, pp. 217-228.

8. Nielsen, Jack N., and Kaatari, George E.: Method for Estimating Lift Interference of Wing-Body Combinations at Supersonic Speeds. NACA RM A51J04, 1951.

9. Lagerstrom, P. A., and Van Dyke, M. D.: General Considerations about Planar and Non-Planer Lifting Systems. Rep. No. SM-13432, Douglas Aircraft Co., Inc., June 1949.

10. Beskin, L.: Determination of Upwash around a Body of Revolution at Supersonic Velocities. Rep. No. APL/JHU-CM-251, The John Hopkins Univ., Appl. Phys. Lab., May 27, 1946.

11. Tsien, Hsue-Shen: Supersonic Flow over an Inclined Body of Revolution. Jour. Aero. Sci., vol. 5, no. 12, Oct. 1938, pp. 480-483.

12. Laitone, E. V.: The Linearized Subsonic and Supersonic Flow about Inclined Slender Bodies of Revolution. Jour. Aero. Sci., vol. 14, no. 11, Nov. 1947, pp. 631-642.

13. Moskowitz, Barry, and Maslen, Stephen H.: Experimental Pressure Distributions over Two Wing-Body Combinations at Mach Number 1.9. NACA RM E50J09, 1951.

14. Puckett, Allen E.: Supersonic Wave Drag of Thin Airfoils. Jour. Aero. Sci., vol. 13, no. 9, Sept. 1946, pp. 475-484.

15. Evvard, John C.: Use of Source Distributions for Evaluating Theoretical Aerodynamics of Thin Finite Wings at Supersonic Speeds. NACA Rep. 951, 1950.

16. Sager, B. F., Kutschinski, C. R., and Goldbaum, G. C.: Sparrow 13-D - Analysis of Force and Moment Characteristics from Supersonic Wind-Tunnel Tests of a 13.5-Percent-Scale Model. Rep. No. SM-13631, Douglas Aircraft Co., Inc., March 17, 1950.

17. Dorrance, W. H.: Body-Tail Interference in Supersonic Flow Including an Example Application. Rep. No. UMM-38, Aero. Res. Center, Univ. of Michigan, Aug. 1949.

18. Jaeger, B. F., and Brown, A. E.: The Aerodynamic Characteristics at Mach Number 2.0 of 14- and 18-Caliber Fin-Stabilized Rockets with Varying Body and Fin Parameters. NAVORD Rep. 1211, U.S. Naval Ord. Test Station, Inyokern, Calif., Jan. 20, 1950.

19. Harshman, J., and Uddenberg, R. C.: Supersonic Wind Tunnel Tests of GAPA Models at a Mach Number of 1.28 in the Aberdeen Tunnel. Doc. No. D-7817, Boeing Aircraft Co., Aug. 2, 1946.

20. Uddenberg, R. C.: Supersonic Wind Tunnel Tests of GAPA Models at a Mach Number of 1.72 in the Aberdeen Tunnel. Doc. No. D-7818, Boeing Aircraft Co., Dec. 1946.

21. Nielson, Jack N., Katzen, Elliott D., and Tang, Kenneth K.: Lift and Pitching-Moment Interference between a Pointed Cylindrical Body and Triangular Wings of Various Aspect Ratios at Mach Numbers of 1.50 and 2.02. NACA RM A50F06, 1950.

22. Hall, Albert W., and Morris, Garland J.: Aerodynamic Characteristics at a Mach Number of 1.25 of a 6-Percent-Thick Triangular Wing and 6- and 9-Percent-Thick Triangular Wings in Combination with a Fuselage. Wing Aspect Ratio 2.31, Biconvex Airfoil Sections. NACA RM L50D05, 1950.

23. Flake, H. M.: Supersonic Wind Tunnel Tests of a 0.020-Scale Model of the NA-705 Missile at Mach Number 2.87 to Determine Effect of Aspect Ratio and Planform of Wings on the Aerodynamic Characteristics of Wing Plus Body. Rep. No. AL-1156, North American Aviation, Inc., Oct. 25, 1950.

24. Fischer, H. S.: Supersonic Wind-Tunnel Tests of a 0.075-Scale Model of the Nike 482 Missile. Rep. No. SM-13848, Douglas Aircraft Co., Inc., Nov. 27, 1950.

25. Ulmann, Edward F., and Dunning, Robert W.: Some Effects of Fin Plan Form on the Static Stability of Fin-Body Combinations at Mach Number 4.06. NACA RM L52D15a, 1952.

26. Rainey, Robert W.: Langley 9-Inch Supersonic Tunnel Tests of Several Modifications of a Supersonic Missile Having Tandem Cruciform Lifting Surfaces. Three-Component Data Results of Models Having Ratios of Wing Span to Tail Span Equal to and Less than 1 and Some Static Rolling-Moment Data. NACA RM L50G07, 1951.

27. Grigsby, Carl E.: Tests at Mach Number 1.62 of a Series of Missile Configurations Having Tandem Cruciform Lifting Surfaces. NACA RM L51J15, 1952.

Figure 1.- The superposition scheme of Lagerstrom and Van Dyke.

(b) Triangular wing.

(a) Rectangular wing.

Figure 2.- Notation.

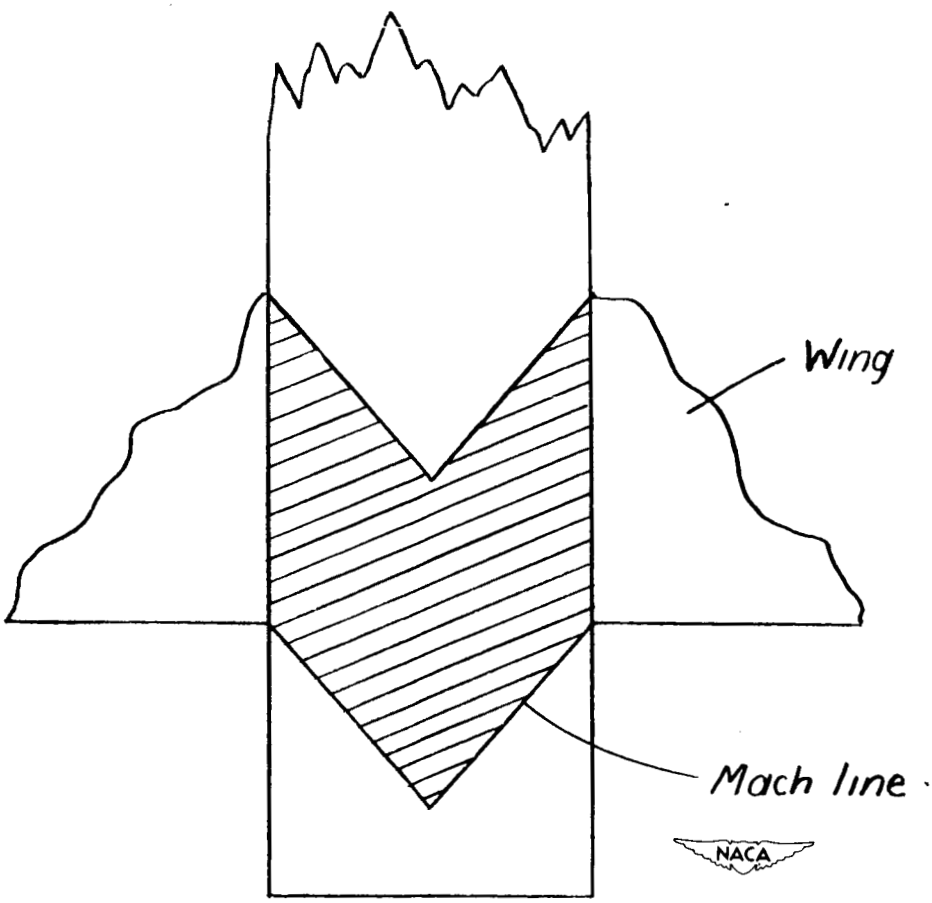

Figure 3.- Area of the flat-plate body within which the lift is assumed to act.

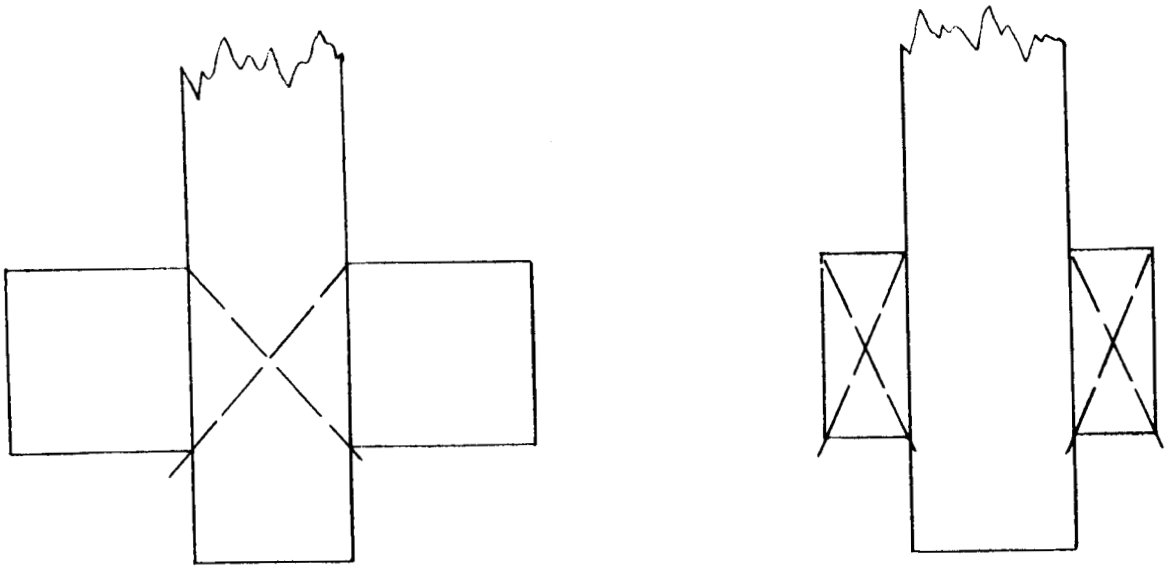

$\beta A\frac{a}{s} = 1$

$\beta A(1 - \frac{a}{s}) = 2$

(a) Rectangular wing.

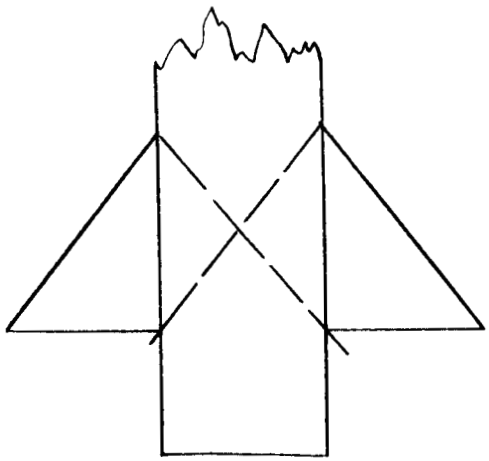

$\frac{a}{s}(1 + 2\beta m) = 1$

(b) Triangular wing.

Figure 4.- Limiting cases for calculations.

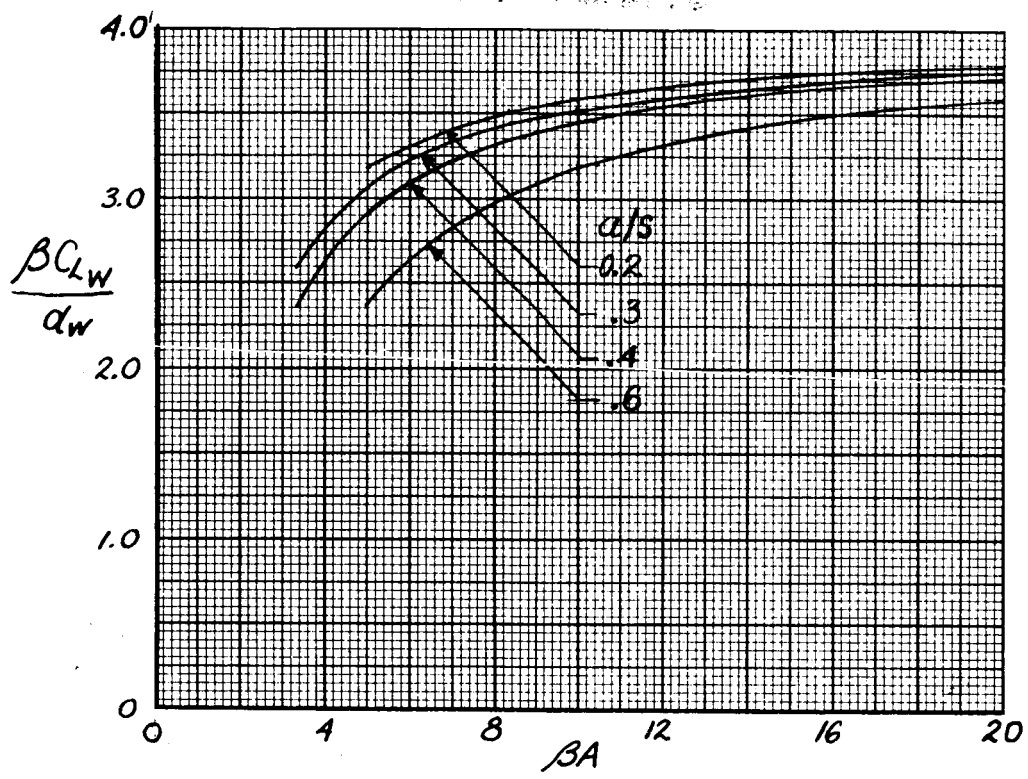

(a) Lift on the wing due to wing angle of attack.

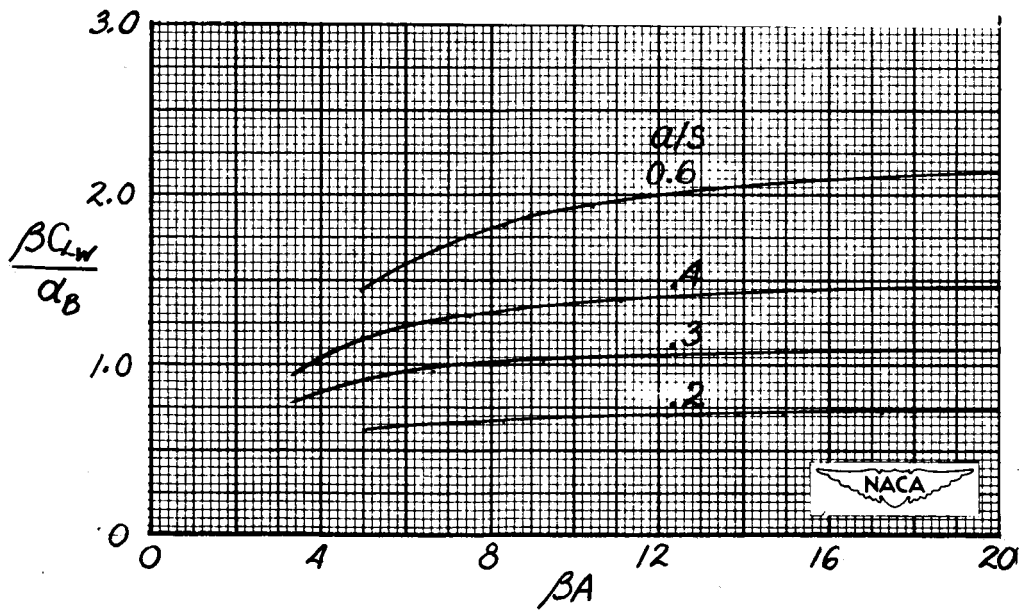

(b) Lift on the wing due to body upwash.

Figure 5.- Lift on wing for wing-body combinations with rectangular wings.

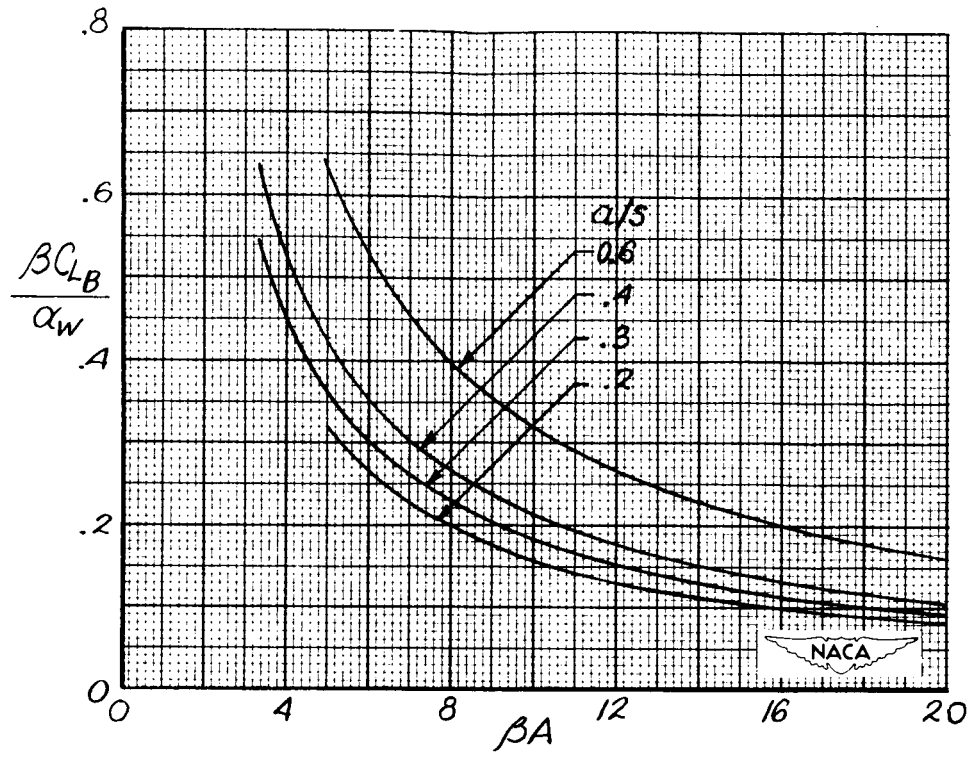

(a) Lift on the body due to wing angle of attack.

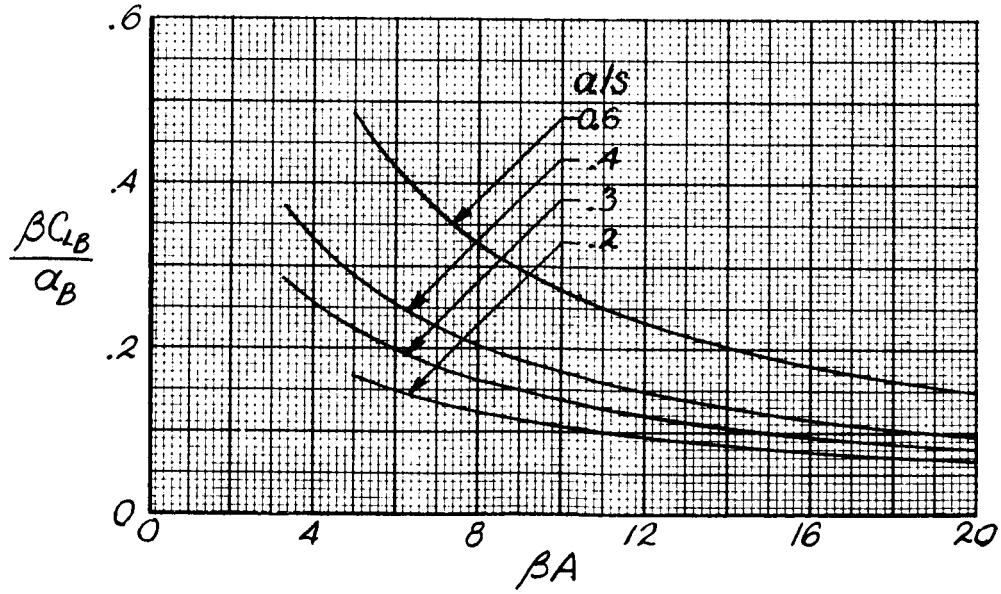

(b) Lift on the body due to body upwash.

Figure 6.- Lift on body for wing-body combinations with rectangular wings and no afterbodies.

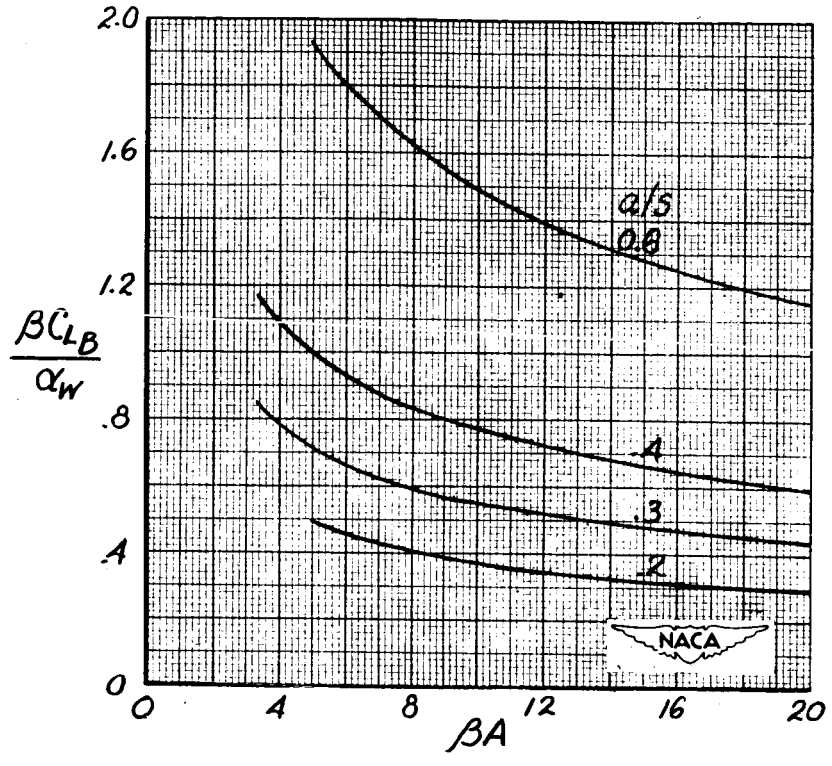

(a) Lift on the body due to wing angle of attack.

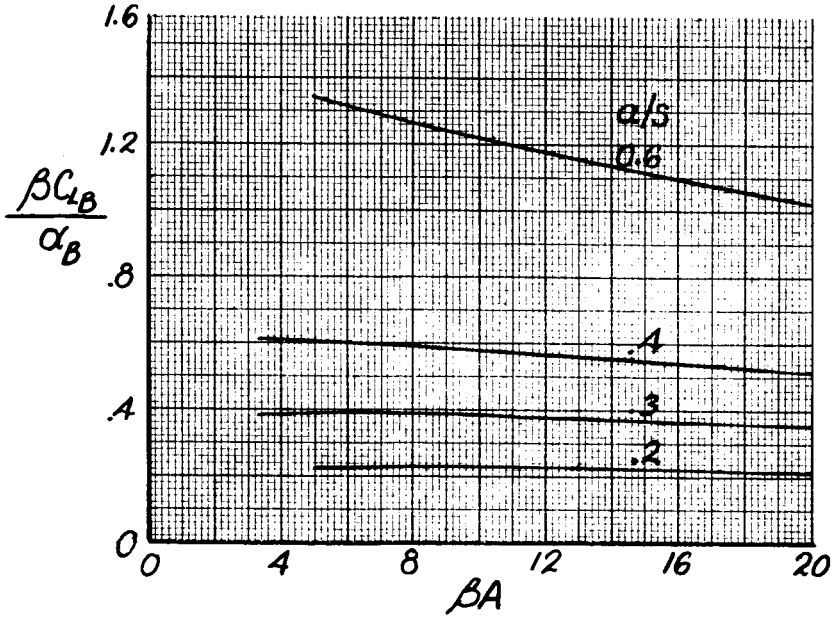

(b) Lift on the body due to body upwash.

Figure 7.- Lift on body for wing-body combinations with rectangular wings and long afterbodies.

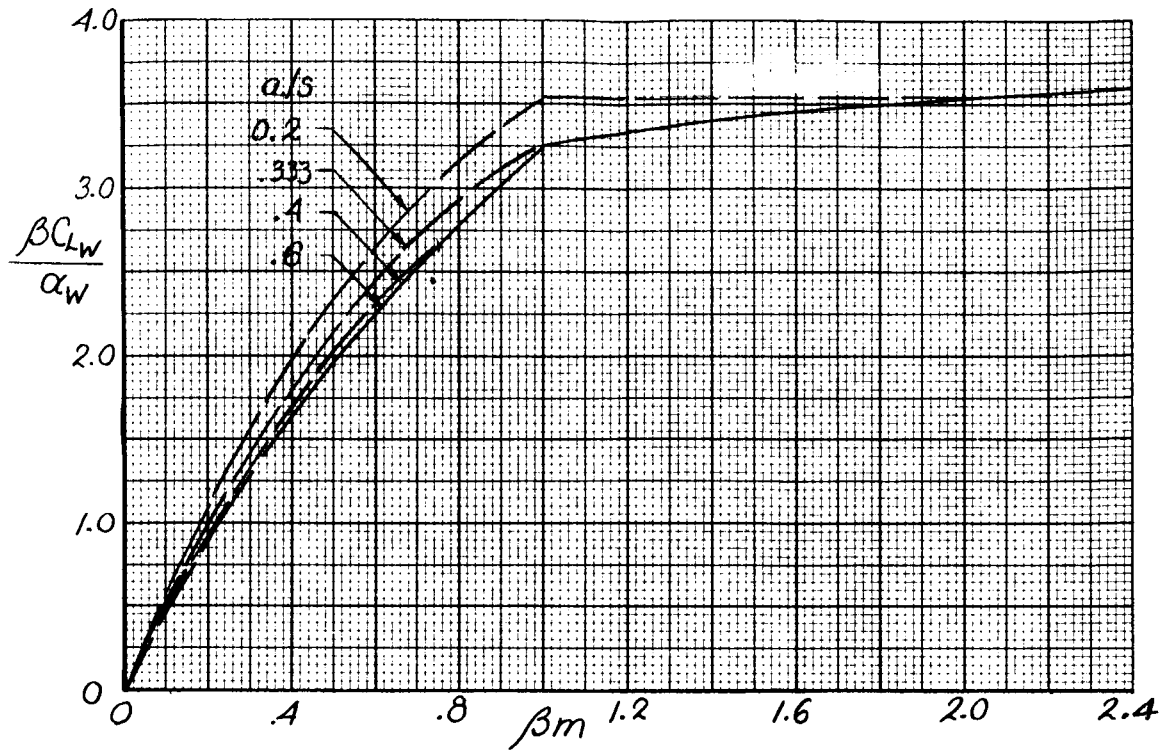

(a) Lift on the wing due to wing angle of attack.

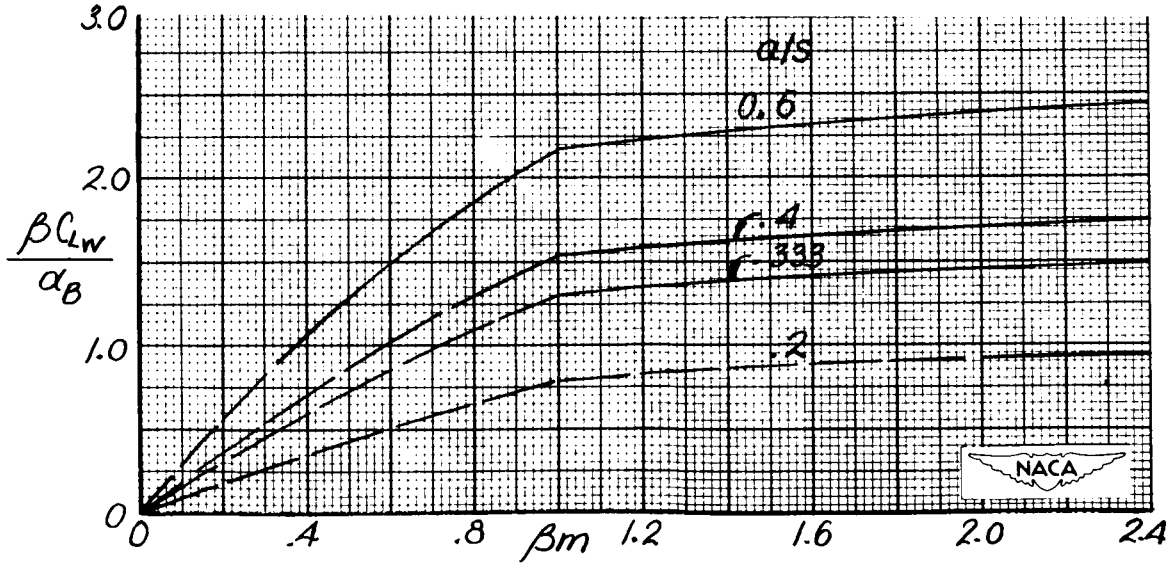

(b) Lift on the wing due to body upwash.

Figure 8.- Lift on wing for wing-body combinations with triangular wings.

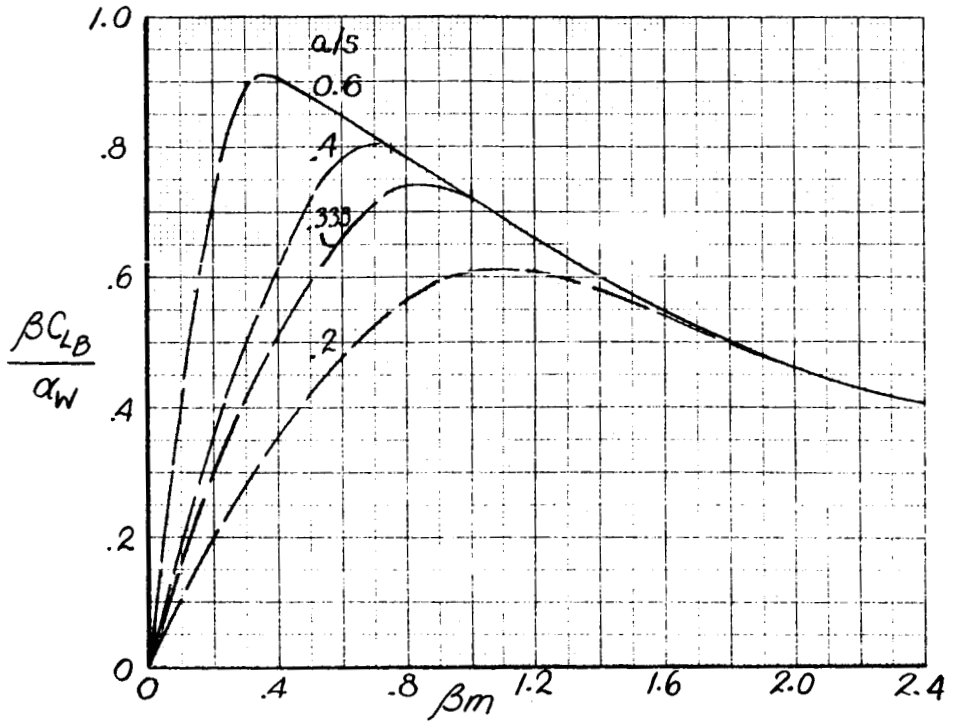

(a) Lift on the body due to wing angle of attack.

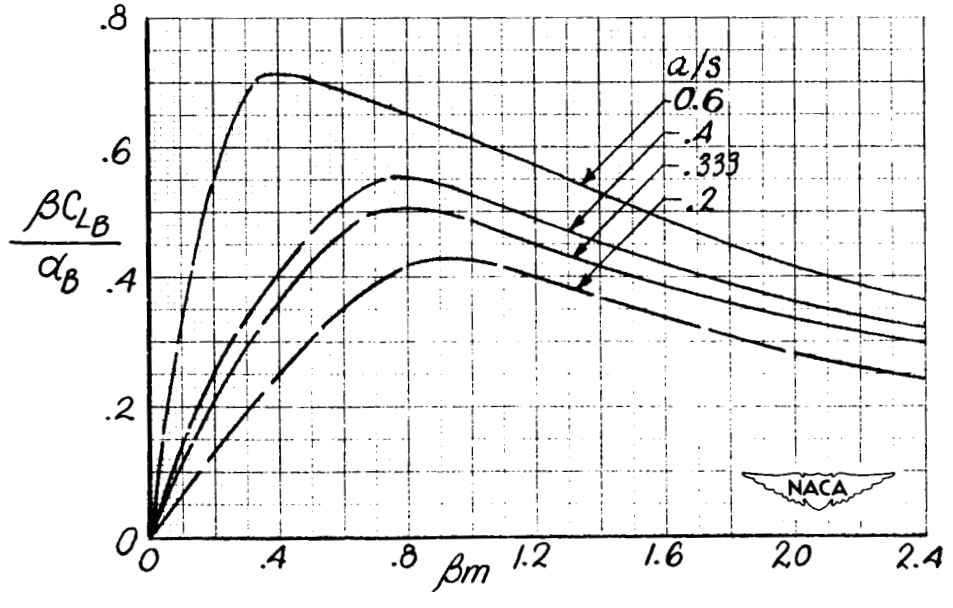

(b) Lift on the body due to body upwash.

Figure 9.- Lift on body for wing-body combinations with triangular wings and no afterbodies.

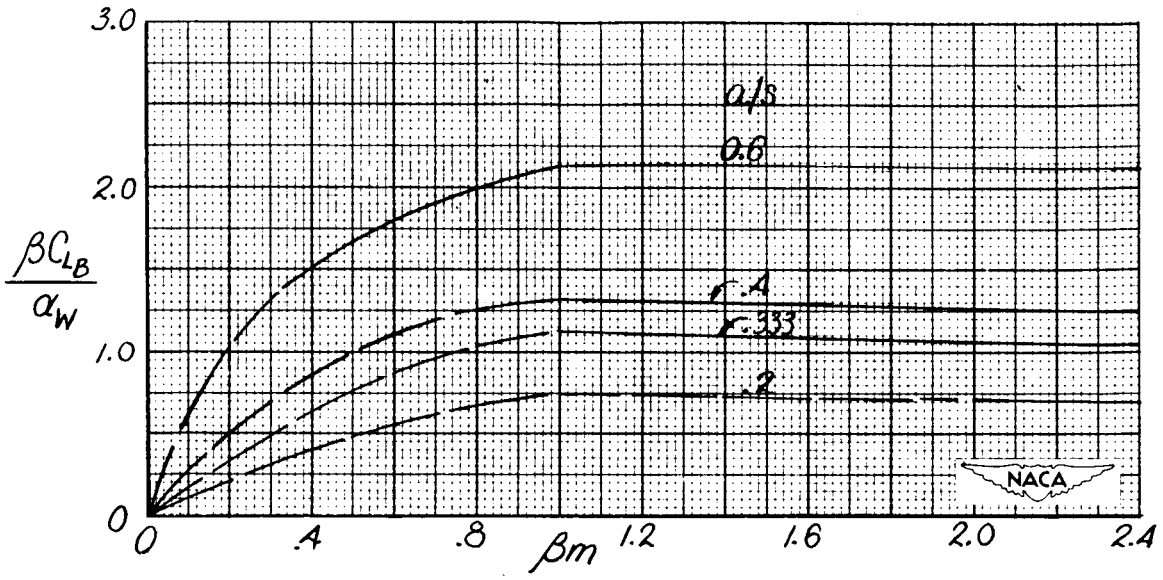

(a) Lift on the body due to wing angle of attack.

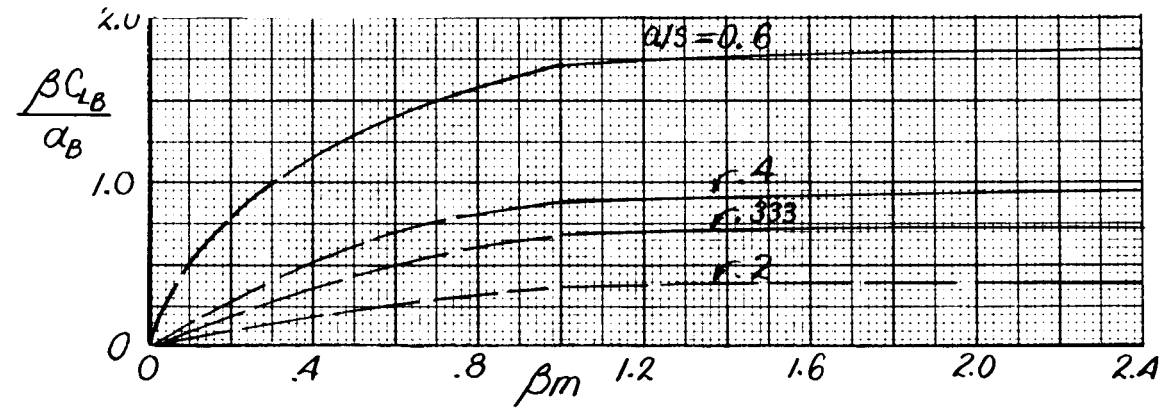

(b) Lift on the body due to body upwash.

Figure 10.- Lift on body for wing-body combinations with triangular wings and long afterbodies.

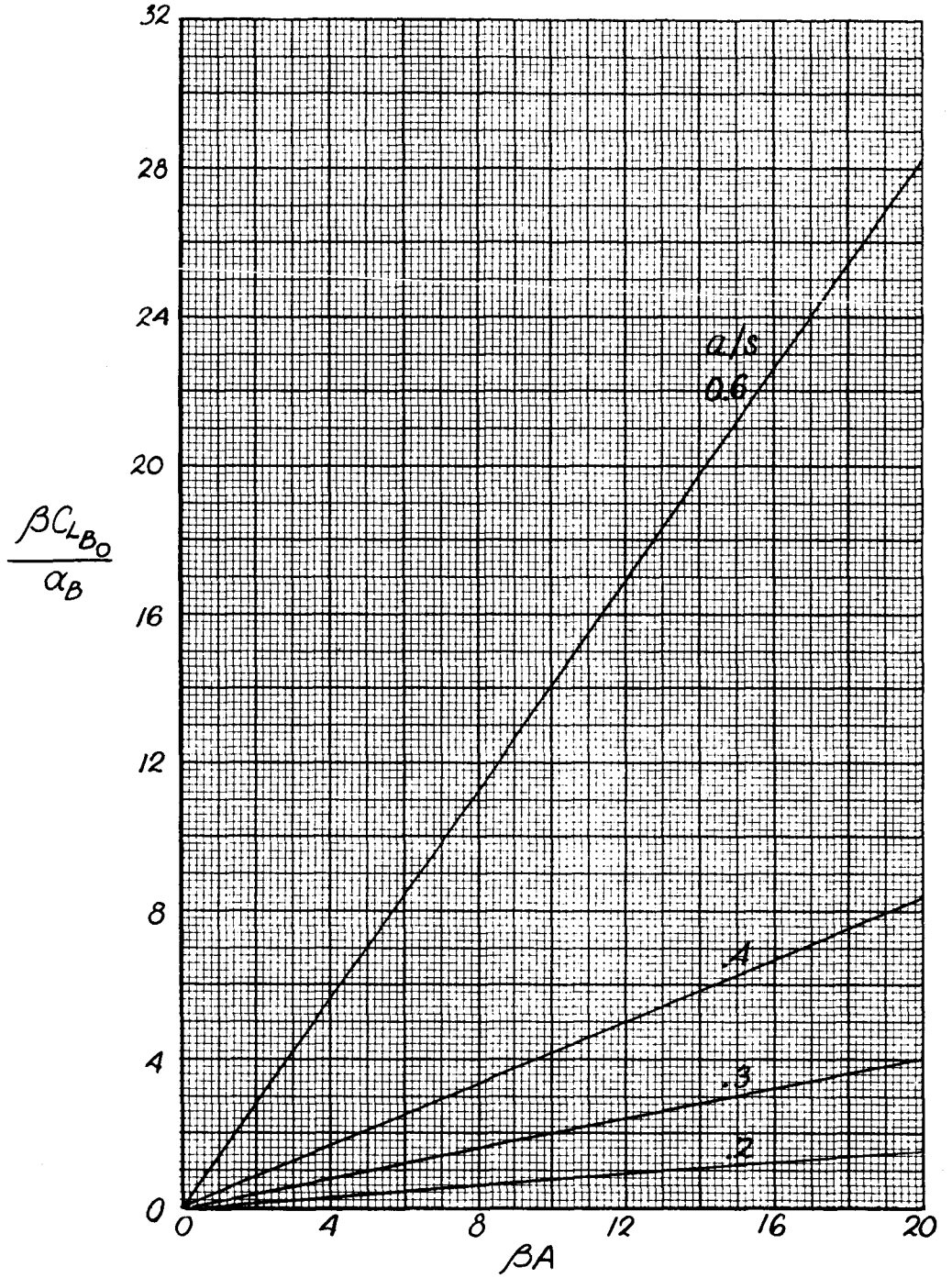

(a) Rectangular wing. $\frac{\beta C_{L_{B_o}}}{\alpha_B} = \frac{\pi}{2} \beta A \frac{(a/s)^2}{1 - \frac{a}{s}}$.

Figure 11.- Lift of isolated body. Lift coefficient based on exposed wing area.

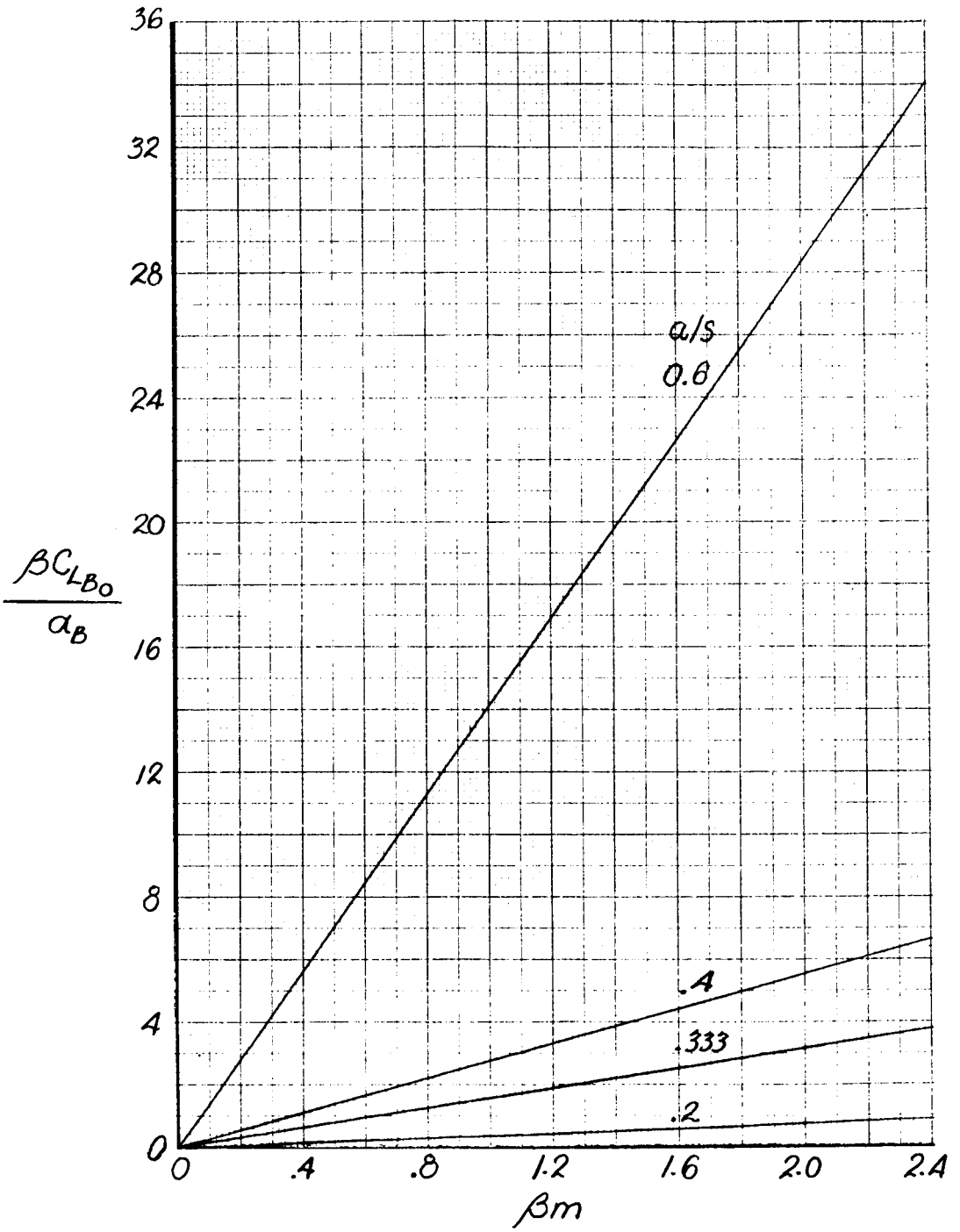

(b) Triangular wing. $\frac{\beta C_{L_{B_o}}}{\alpha_B} = 2\pi\beta m\left(\frac{a/s}{1 - \frac{a}{s}}\right)^2$.

Figure 11.- Concluded.

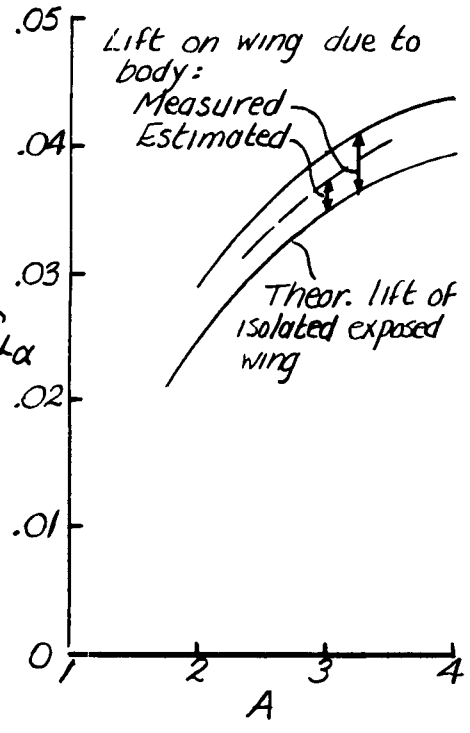

(a) M = 1.62.

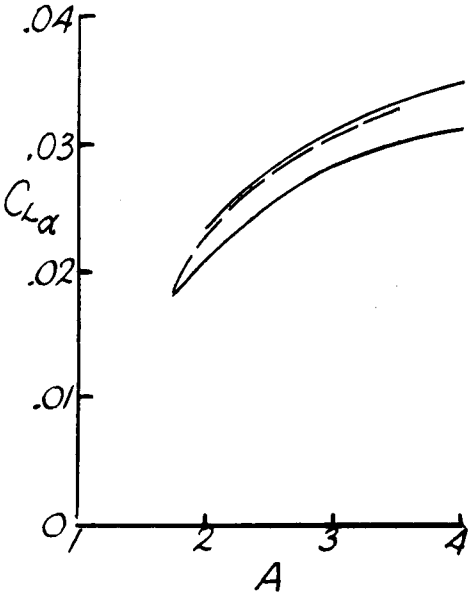

(b) M = 1.93.

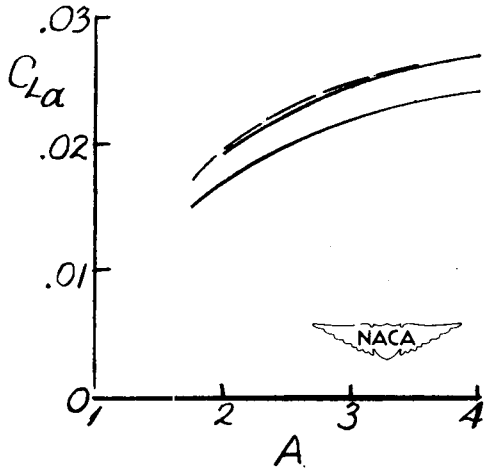

(c) M = 2.40.

Figure 12.- Comparison with Langley 9-inch supersonic-tunnel results for rectangular-wing case. Lift on wing due to body. Coefficients based on total wing area; α in degrees.

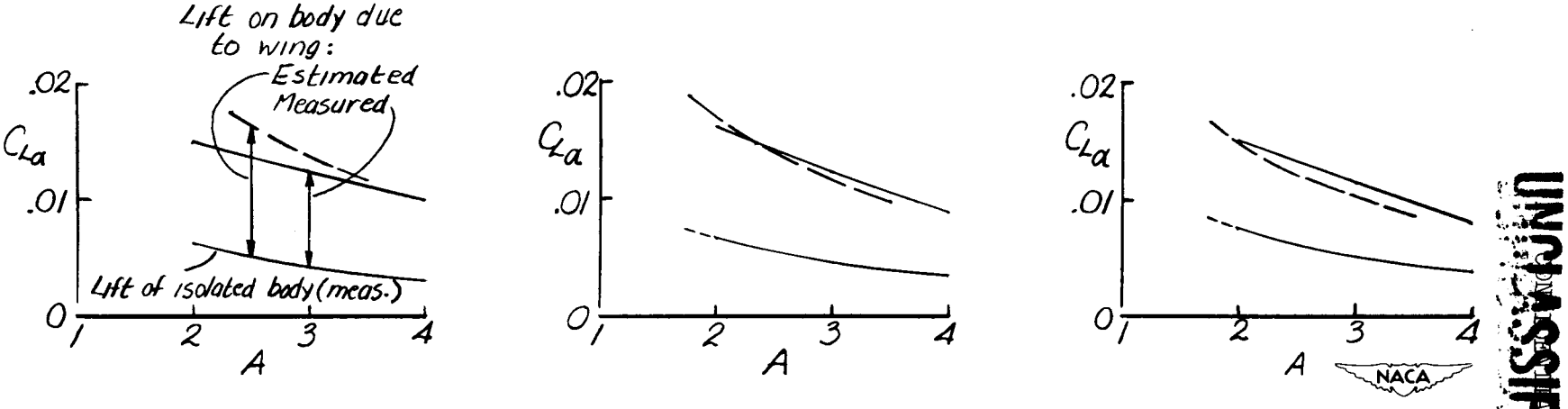

(a) M = 1.62. (b) M = 1.93. (c) M = 2.40.

Figure 13.- Comparison with Langley 9-inch supersonic-tunnel results for rectangular-wing case. Lift on body due to wing. Coefficients based on total wing area; α in degrees.

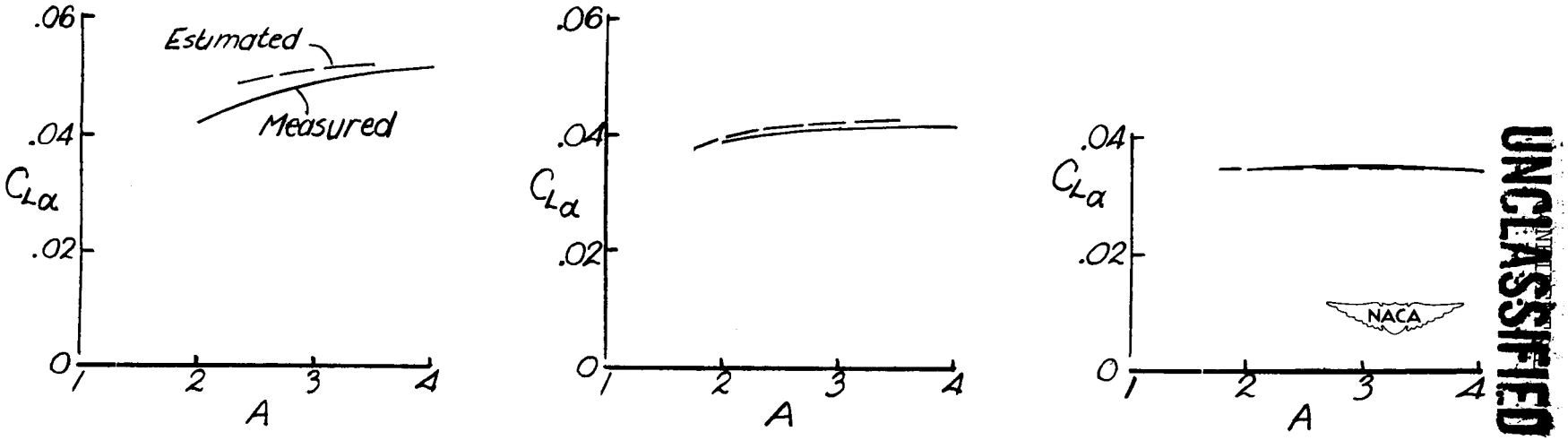

(a) M = 1.62. (b) M = 1.93. (c) M = 2.40.

Figure 14.- Comparison with Langley 9-inch supersonic-tunnel results for rectangular-wing case. Total lift of wing-body combination. Coefficients based on total wing area; α in degrees.

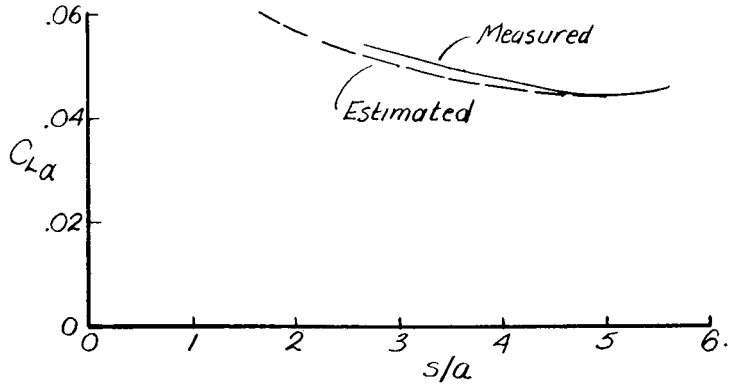

(a) M = 1.62.

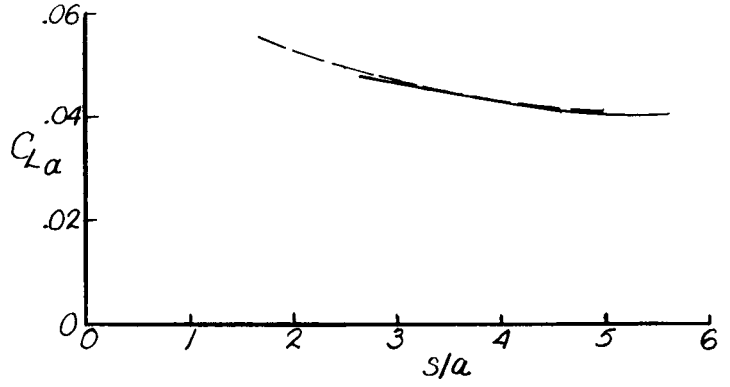

(b) M = 1.93.

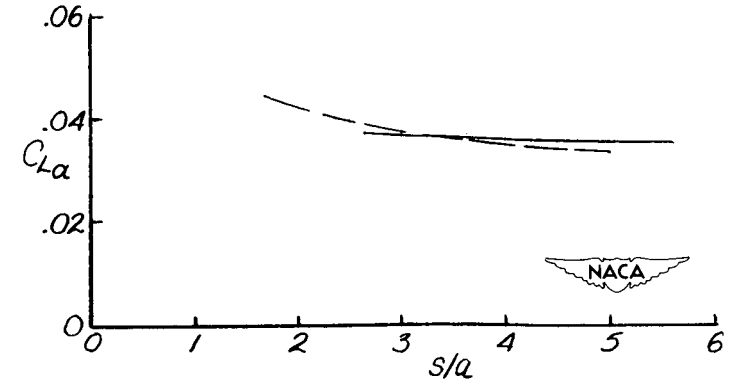

(c) M = 2.40.

Figure 15.- Comparison with Langley 9-inch supersonic-tunnel results for lift on triangular wing in presence of body. Sweepback angle of leading edge, 60°. Coefficients based on exposed wing area; α in degrees.

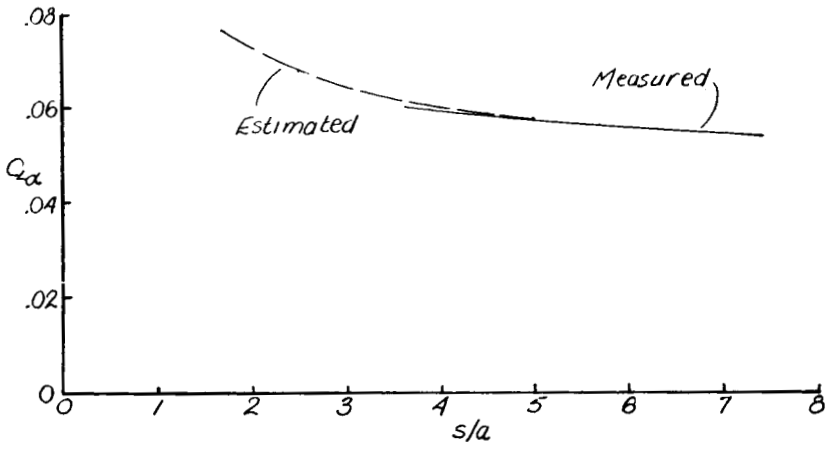

(a) M = 1.62.

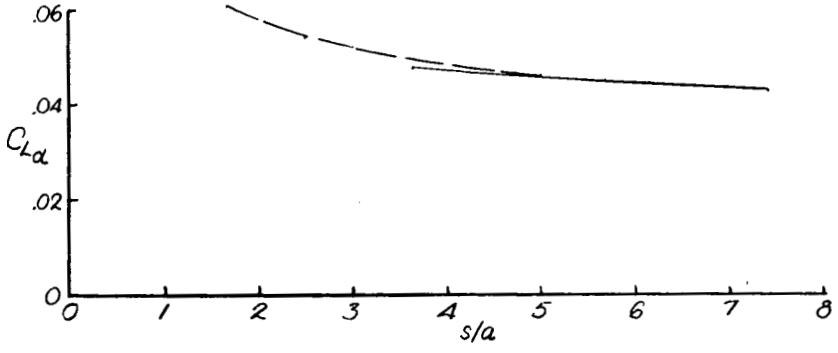

(b) M = 1.93.

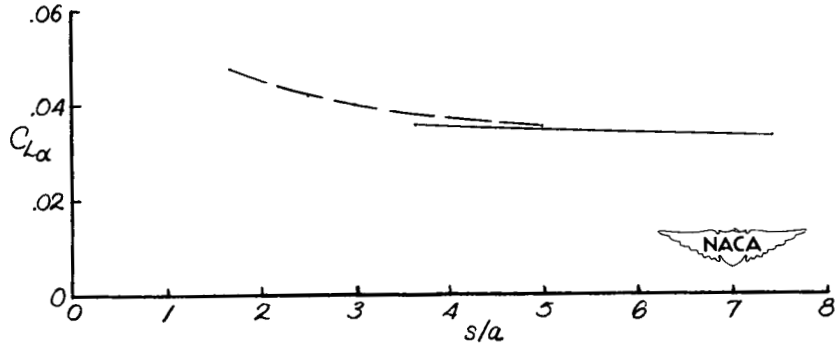

(c) M = 2.40.

Figure 16.- Comparison with Langley 9-inch supersonic-tunnel results for lift on triangular wing in presence of body. Sweepback angle of leading edge, 45°. Coefficients based on exposed wing area; α in degrees.

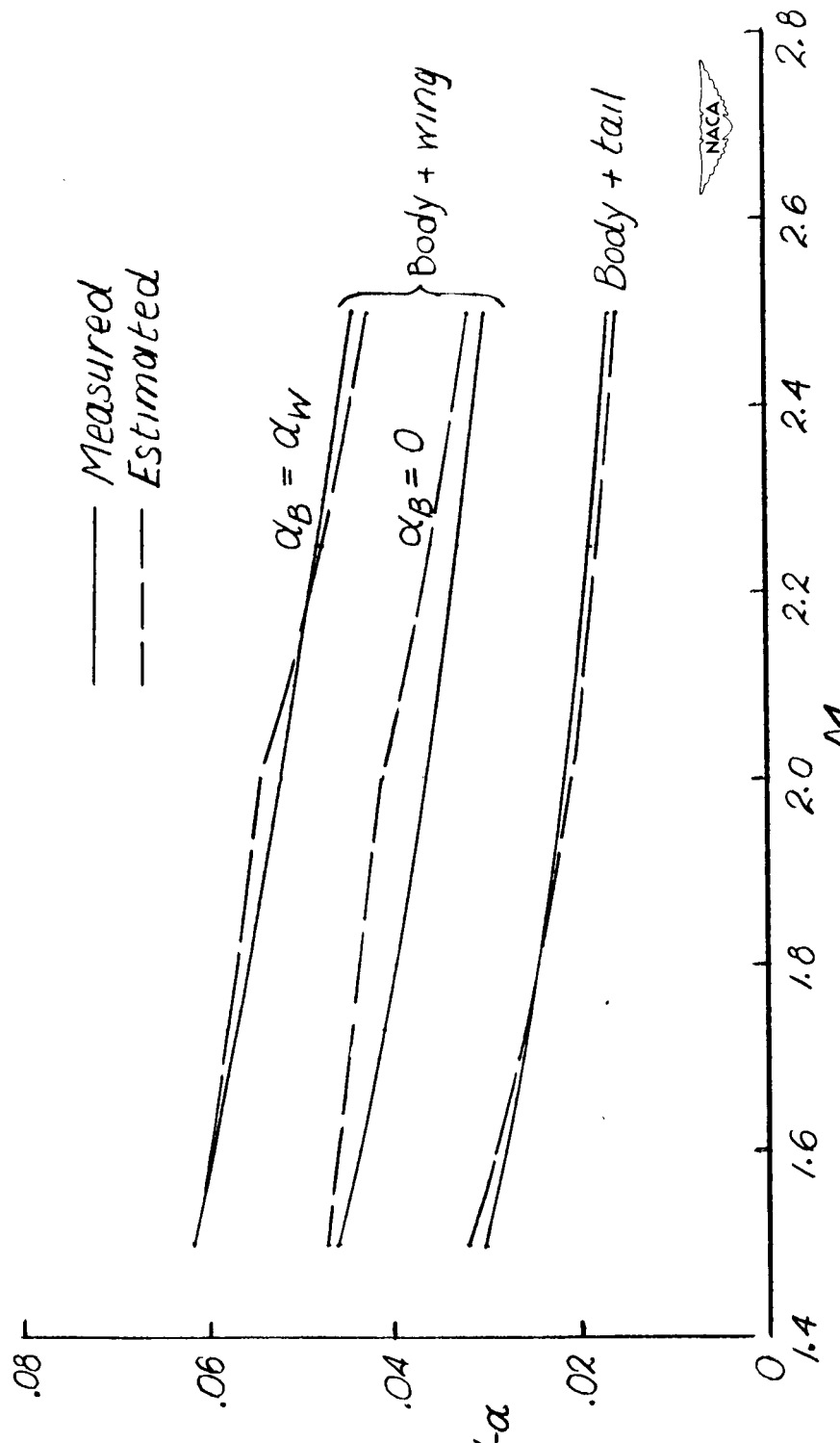

Figure 17.- Comparison with data for model of Sparrow missile. Lift on combination minus lift of isolated body (except for $\alpha_B = 0$ curves).

Coefficients based on exposed wing area; α in degrees.

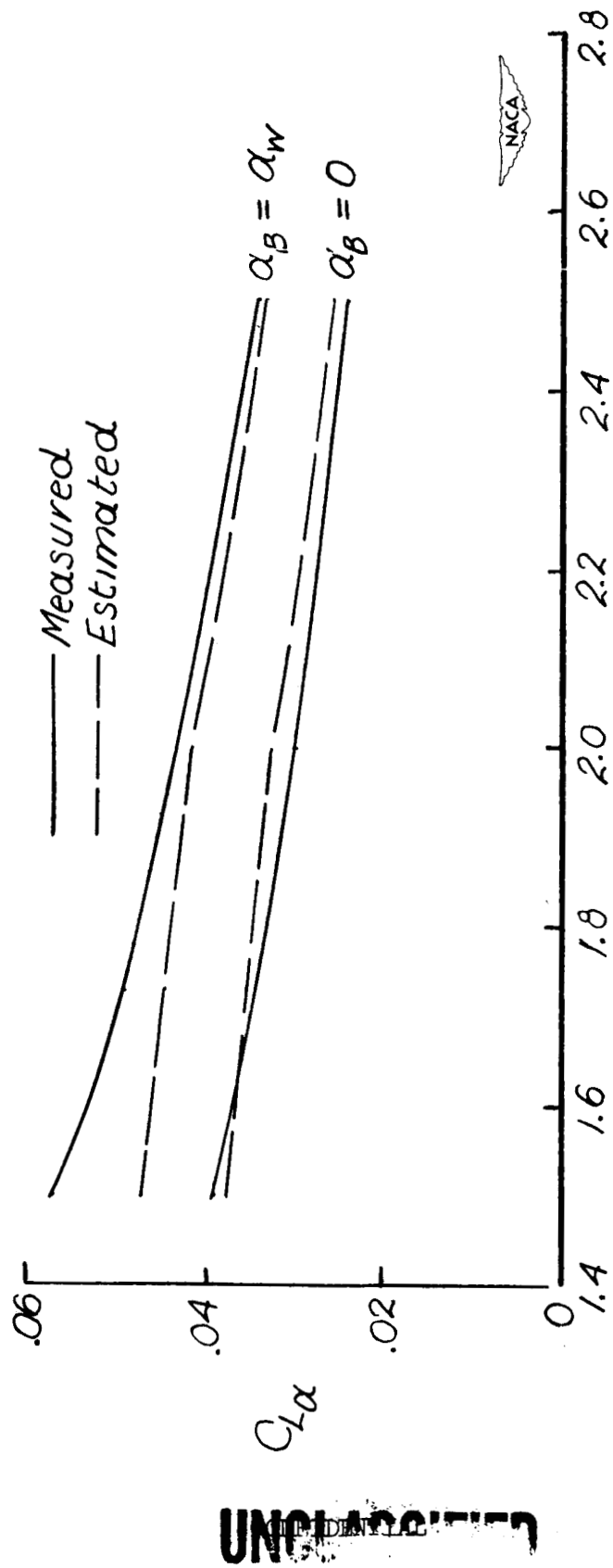

Figure 18.- Comparison with data for model of Sparrow missile. Lift on wing in presence of body. Coefficients based on exposed wing area; α in degrees.

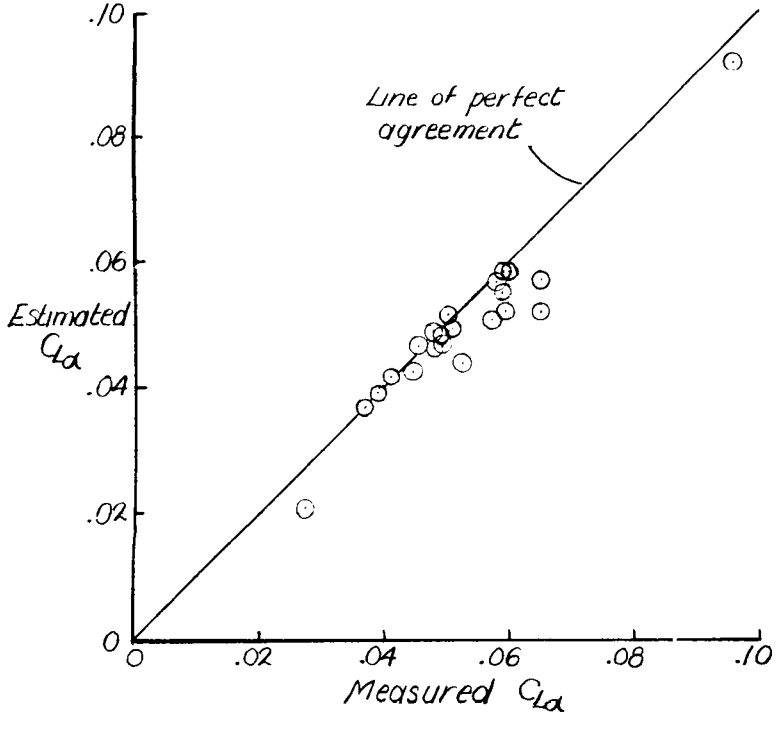

(a) Lift of isolated body subtracted.

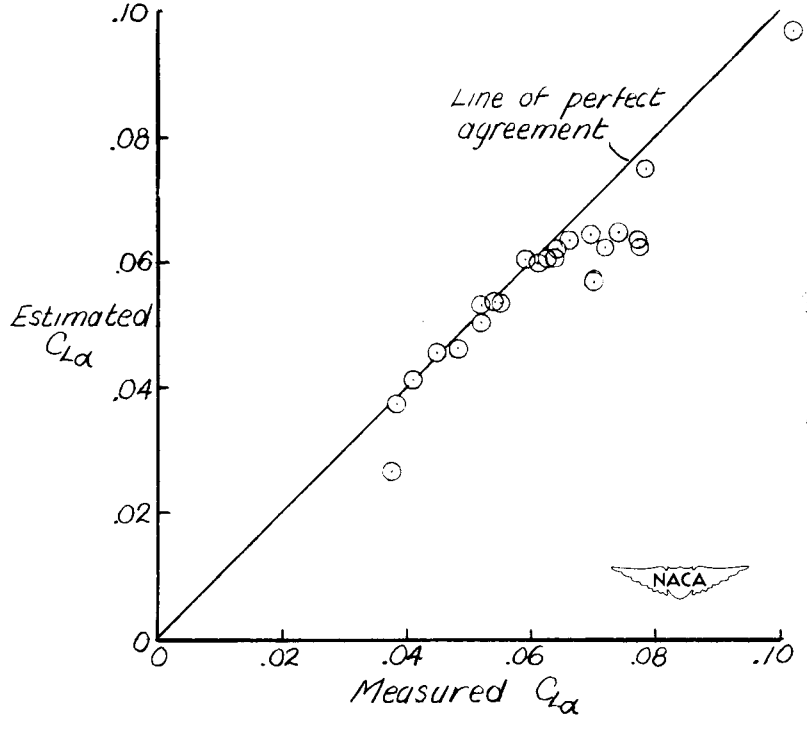

(b) Complete lift.

Figure 19.- Correlation of total lift for 22 wing-body configurations. Rectangular wings. Coefficients based on exposed wing area; α in degrees.

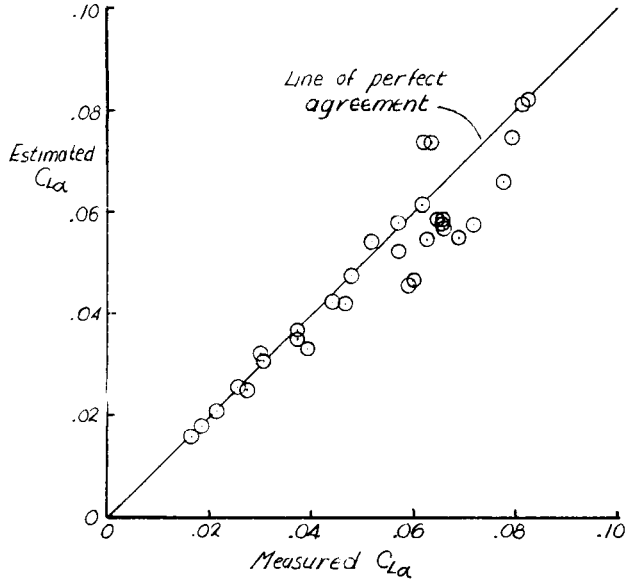

(a) Lift of isolated body subtracted.

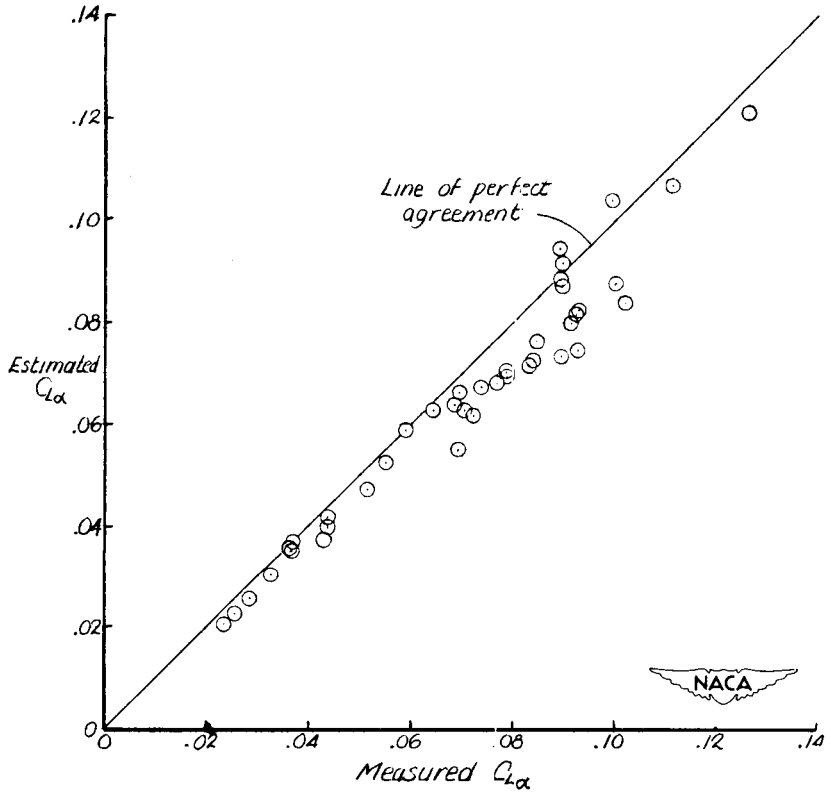

(b) Complete lift.

Figure 20.- Correlation of total lift for 32 wing-body combinations. Triangular wings. Coefficients based on exposed wing area; α in degrees.

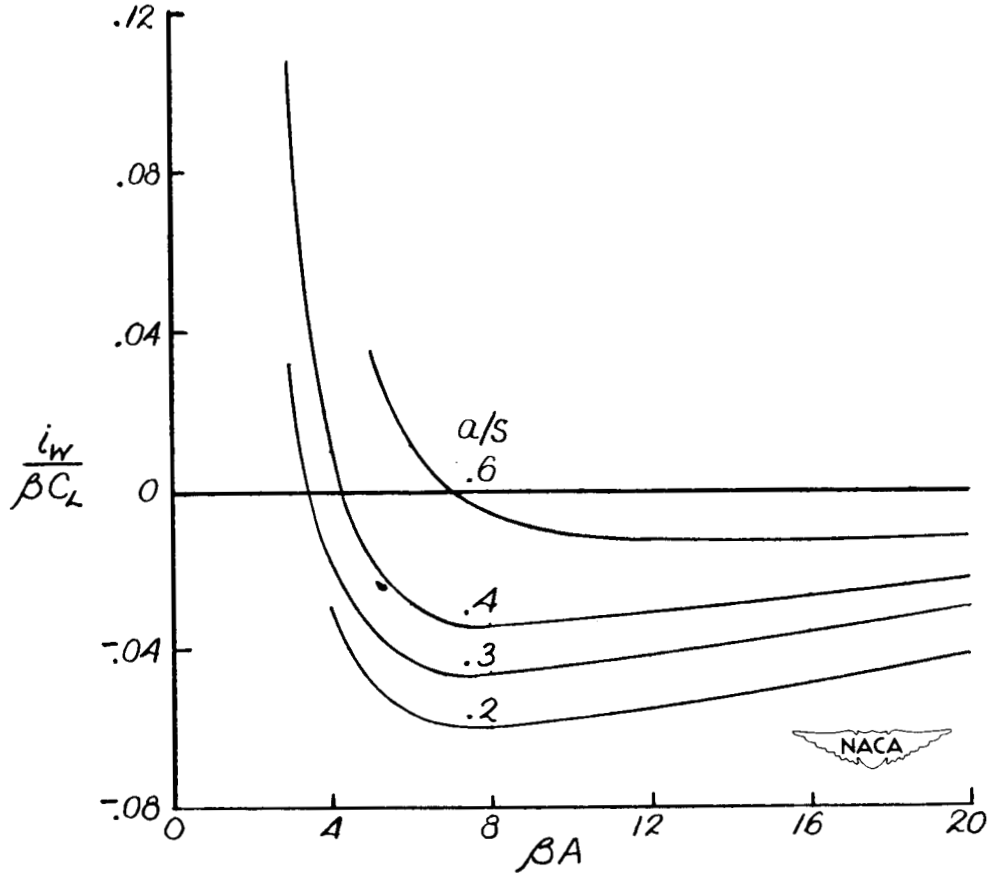

(a) Rectangular wings.

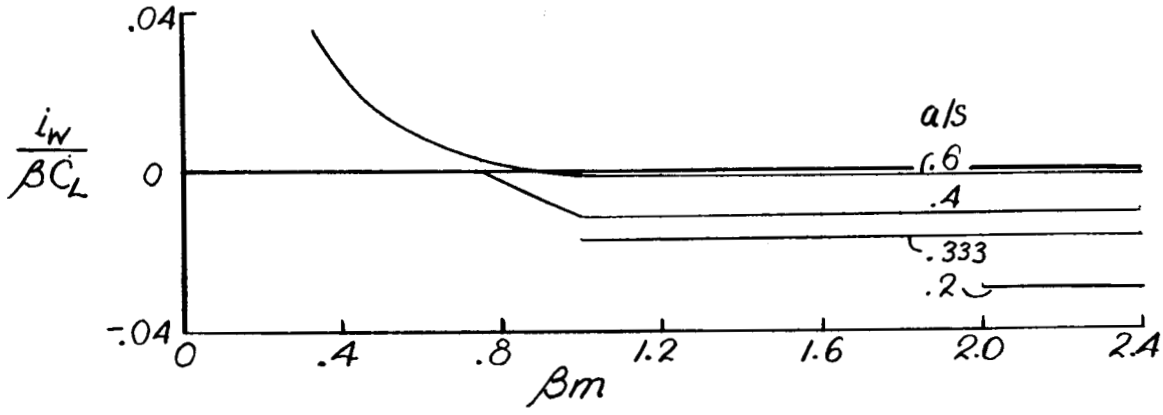

(b) Triangular wings.

Figure 21.- Angle of incidence for minimum drag due to lift.

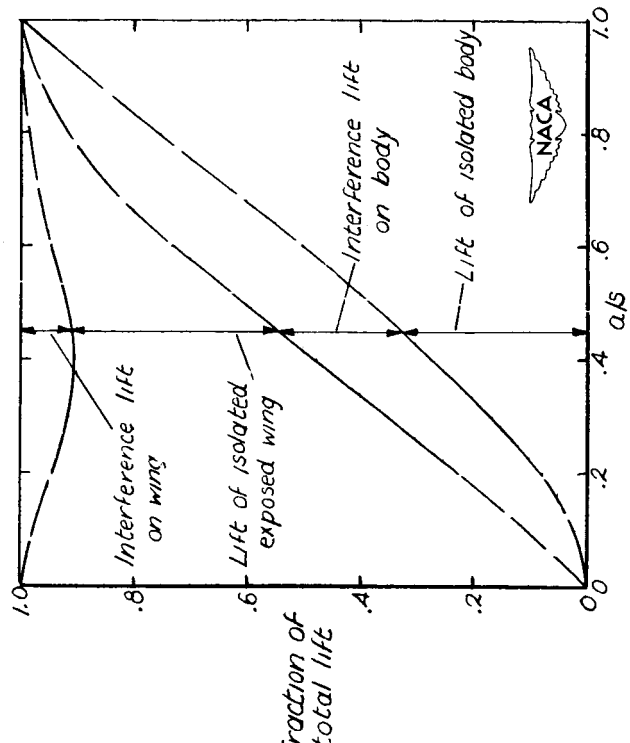

(b) Long afterbody.

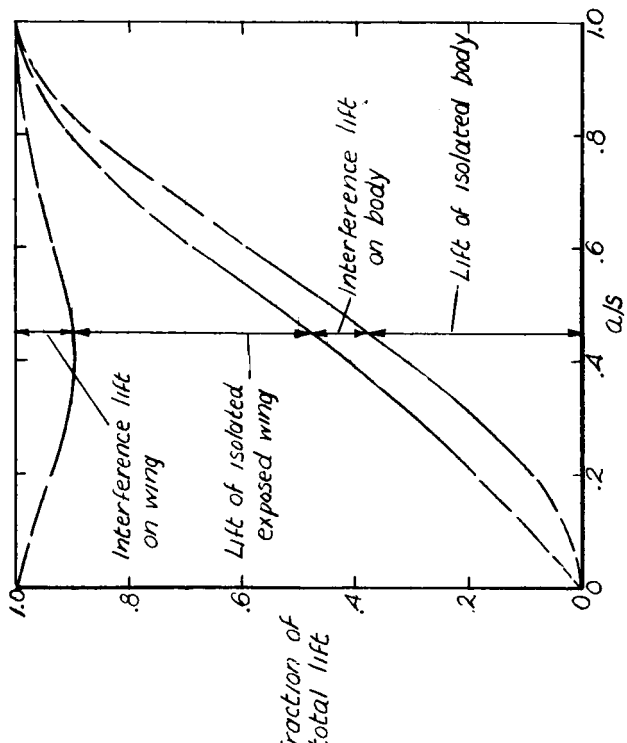

(a) No afterbody.

Figure 22.- Division of lift for wing-body combinations. Rectangular wing; $\beta A = 5$.

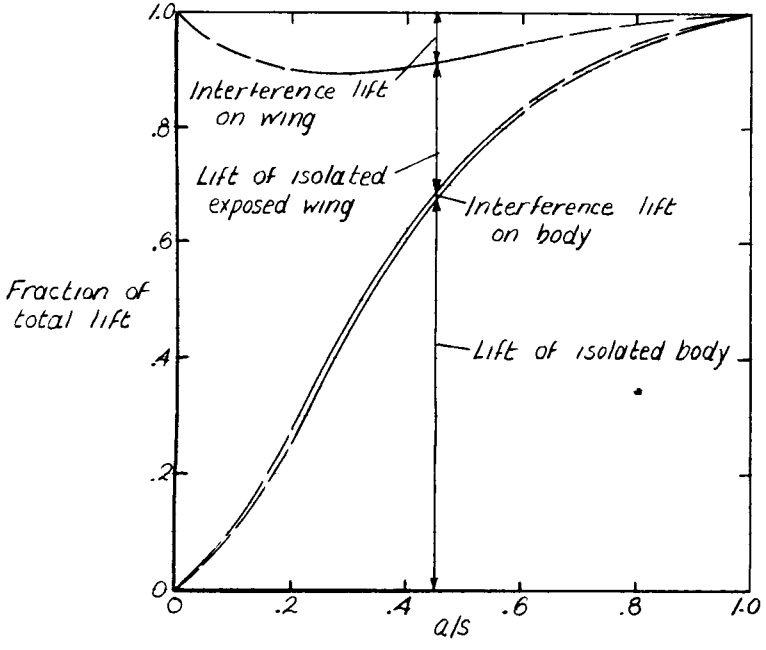

(a) No afterbody.

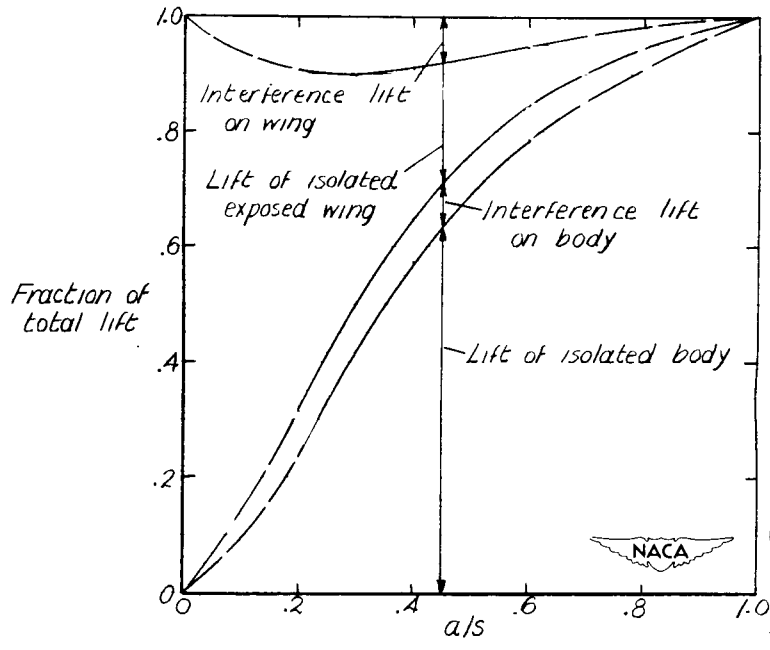

(b) Long afterbody.

Figure 23.- Division of lift for wing-body combinations. Rectangular wing; βA = 20.

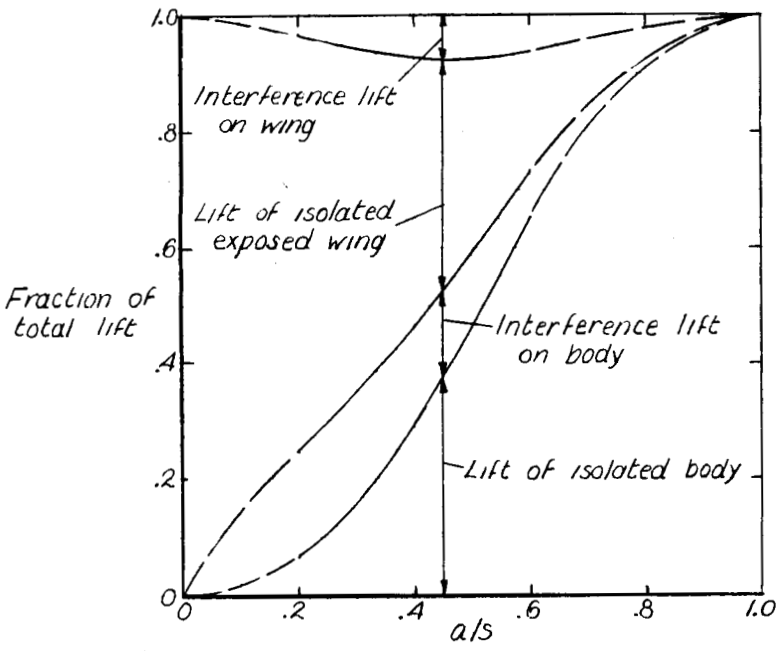

(a) No afterbody.

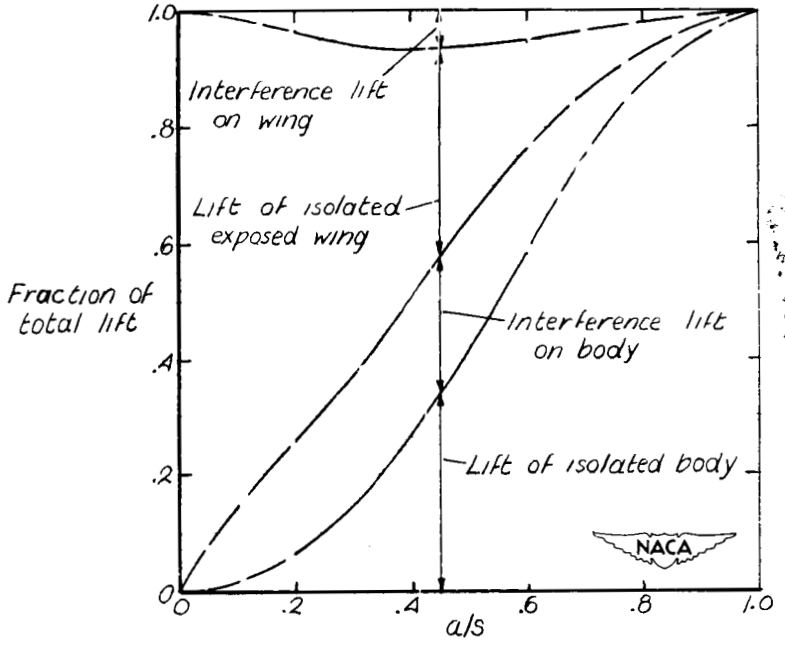

(b) Long afterbody.

Figure 24.- Division of lift for wing-body combinations. Triangular wing; $\beta m = 0.8$.

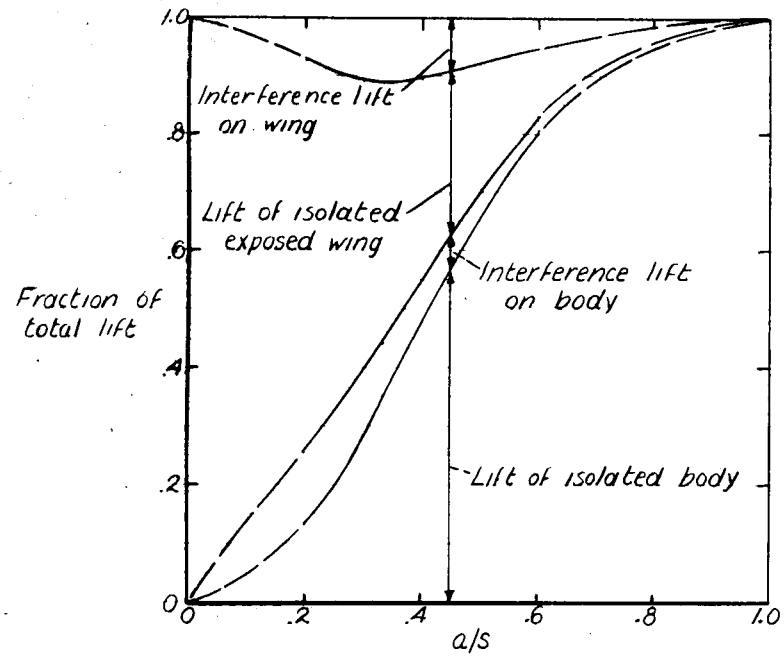

(a) No afterbody.

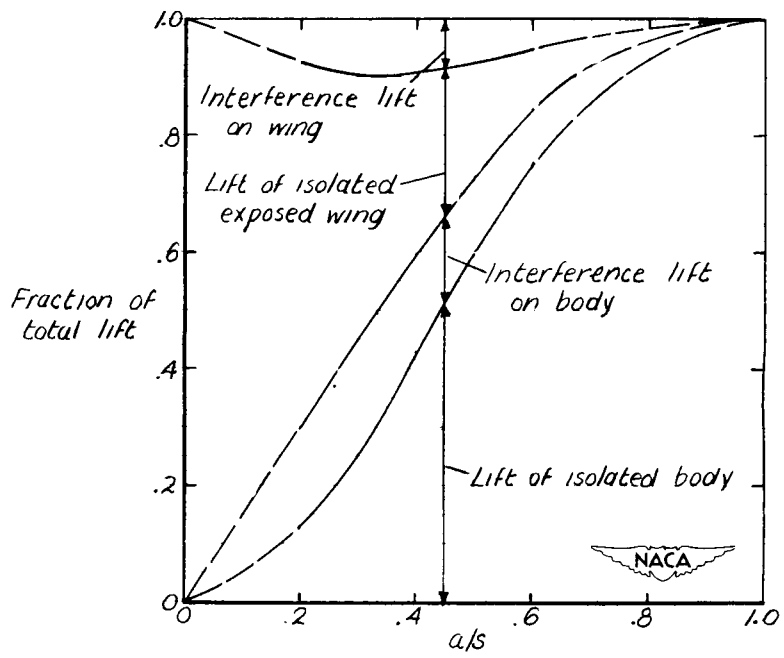

(b) Long afterbody.

Figure 25.- Division of lift for wing-body combinations. Triangular wing; $\beta m = 2.0$.

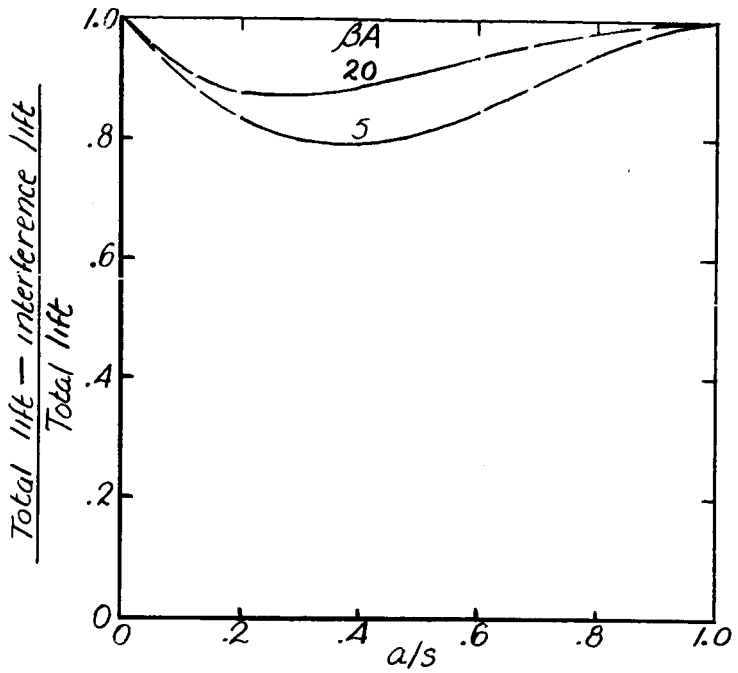

(a) No afterbody.

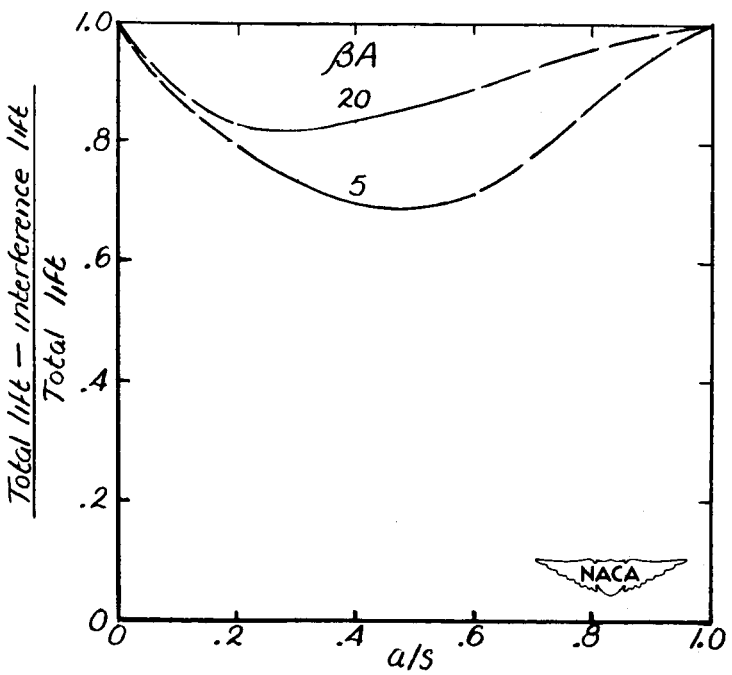

(b) Long afterbody.

Figure 26.- Interference lift for wing-body combinations with rectangular wings.

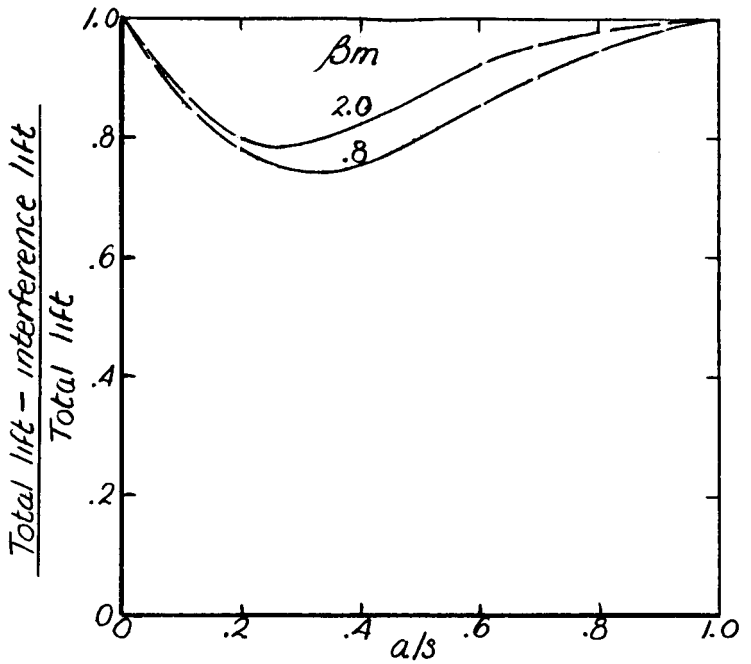

(a) No afterbody.

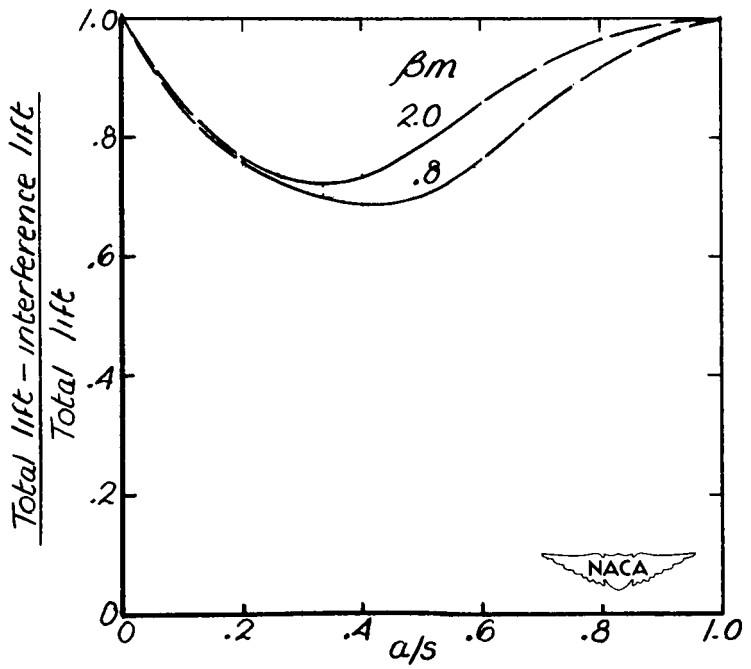

(b) Long afterbody.

Figure 27.- Interference lift for wing-body combinations with triangular wings.

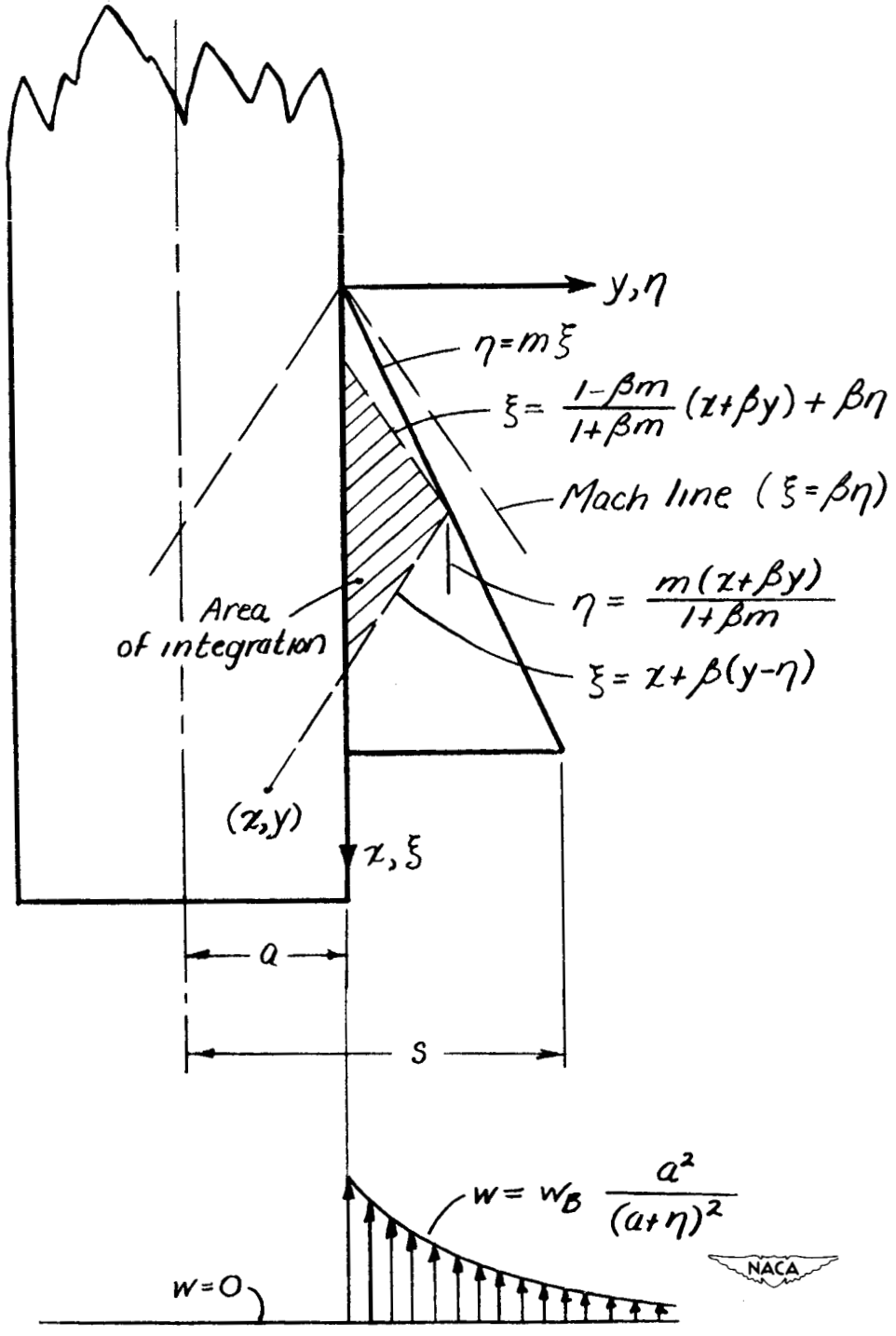

Figure 28.- Setup for integration described in appendix.

NACA-Langley - 9-16-52 - 350